The Role of ROCK in Colon Cancer Invasion Using Three-Dimensional Collagen I Microenvironments

BY

RAMANA VENKATA VISHNUBHOTLA
B.S. University of Michigan, 2002

THESIS

Submitted as partial fulfillment of the requirements
for the degree of Doctor of Philosophy in Bioengineering
in the Graduate College of the
University of Illinois at Chicago, 2012

Chicago, Illinois

Defense Committee:

Michael Cho, Chair
Sarah C. Glover, University of Florida, Advisor
Jun Cheng
Seungpyo Hong, Biopharmaceutical Sciences
Vitali Metlushko, Electrical and Computer Engineering
Gerardo Morfini, Anatomy and Cell Biology

DEDICATION

I would like to dedicate my doctoral dissertation to my parents: Dr. Raghunadha Sarma and Rajeswari who instilled in me the value of education and always supported me in my pursuit of higher education. I would also like to dedicate this to my late maternal grandfather Dr. V.V. Somayajulu who passed away May 24, 2011.

ACKNOWLEDGEMENTS

I would first like to acknowledge the contributions of my main dissertation advisor, Dr. Sarah C. Glover, for supporting my project from the initial to final stages. Without her contributions, this project would not have been possible. I would like to especially thank her for all her advice, encouragement, and support throughout the years for which I had the fortune and honor of being her first PhD student.

Next, I would like to thank my co-advisor/committee chairman, Dr. Michael Cho, for his contributions towards my project. I would like to thank him for allowing me to use his laboratory equipment for my project as well as all the advice, support, and guidance he has given me over the years. I would also like to thank my other committee members: Dr. Jun Cheng, Dr. David T. Eddington, Dr. Richard A. Gemeinhart, Dr. Seungpyo Hong, Dr. Vitali Metlushko, Dr. Gerardo Morfini, and Dr. Brenda Russell for the contributions they provided to my project and towards my growth as a scientist.

I would also like to give a special thanks to Dr. Shan Sun and Dr. Igor Titushkin for their guidance and time spent for cell imaging. I would also like to acknowledge the contributions of my labmates: Shruthi Bharadwaj, Marinka Bulic, Chinmay Chauhan, Crystal Foster, Jameela Huq, Victor Nekrasov, and Rebecca Rapier. Finally, I would like to thank Linda Juarez in the UIC EM facility for her work with TEM images.

ACKNOWLEDGEMENTS (continued)

This work was supported by the Elisa Pardee Foundation and the National Institutes of Health (1 RO1 CA113975-A2).

TABLE OF CONTENTS

TABLE OF CONTENTS (continued)

LIST OF TABLES (continued)

LIST OF FIGURES

LIST OF FIGURES (continued)

LIST OF ABBREVIATIONS

AJCC	American Joint Committee on Cancer
BMP-2	Bone Morphogenetic Protein-2
CMTMR	5-(and-6)-(((4-Chloromethyl)Benzoyl)Amino) Tetramethylrhodamine
DAPI	4',6 Diamidino-2-Phenylindole
DGEA	Aspartate-Glycine-Glutamate-Alanine
DMEM	Dulbecco's Modified Eagle Medium
DMSO	Dimethyl Sulfoxide
ECM	Extracellular Matrix
ELISA	Enzyme-Linked Immunosorbent Assay
EMT	Epithelial to Mesenchymal Transition
FBS	Fetal Bovine Serum
FIT-C	Fluorescein Isothiocyanate
GBM	Glioblastoma
HRP	Horseradish Peroxidase
IBD	Inflammatory Bowel Disease
MMP	Matrix-Metalloproteinase
MSC	Mesenchymal Stem Cell
MTT	3-(4,5-Dimethylthiazol-2-yl)-2,5-diphenyltetrazolium bromide
NaOH	Sodium Hydroxide

LIST OF ABBREVIATIONS (continued)

NBF	Neutral Buffered Formalin
PBS	Phosphate Buffered Saline
PLB	Phosphate Lysis Buffer
PVDF	Polyvinyalidene Fluoride
RGD	Arginine-Glycine-Aspartate
ROCK	Rho-Kinase
SDS	Sodium Dodecyl Sulfate
siRNA	Short Interfereing Ribonucleic Acid
TBST	Tris-Buffered Saline Tween-20
TEM	Transmission Electron Microscopy
TGF-β:	Transforming Growth Factor-β
TRIT-C	Tetramethyl Rhodamine Iso-Thiocyanate
VEGF	Vascular Endothelial Growth Factor

SUMMARY

Colon cancer is the third leading cause of cancer-related deaths in the US. As with other cancers the chances of survival greatly increase the earlier the cancer is detected. While current treatments are effective for treating primary tumors, they are not effective in preventing metastasis, or spreading of the tumor to other organs. At the same time, most cancer research has been focused on understanding the biochemistry but much less has been done to sufficiently understand cancer cell invasion within the tumor microenvironment.

To understand cell motility one must understand the interaction between a cell and its surrounding environment. This can be challenging because of the difficulty to recreate such an environment for *in vitro* studies. *In vivo*, cells are attached to other cells and/or an extracellular matrix (ECM). Malignant cancer cells have the ability to invade through tissue barriers and migrate through the ECM. To better understand how colon cancer cells invade through the ECM, we constructed a three-dimensional model with type I collagen, the most abundant ECM component found *in vivo*. This model consisted of creating a type I collagen hydrogel. Cells were seeded onto this gel and allowed to invade, similar to how a tumor would invade into surrounding tissue.

We have seen through histological staining of colonic tumor samples (using antibodies against various markers) that Rho-kinase-II (ROCK-II) is heavily expressed at the tumor leading edge. Therefore, it was important to understand the molecular mechanism by which ROCK-II impacts colon cancer

invasion in a 3D collagen I microenvironment. Using fluorescence microscopy, we found that ROCK-II was expressed heavily in protrusive structures towards the cell periphery in malignant cell lines. Furthermore, the collagen matrix was absent adjacent to these structures. We were able to confirm these structures to be invadopodia using transmission electron microscopy (TEM). The absence of ROCK-II expression resulted in significantly reduced invasion and matrix-metalloproteinase (MMP) expression in malignant colonocytes. Taken together, this data strongly supports the claim that ROCK-II is associated with colon cancer invasion and linked to invadopodia formation. It also demonstrates that reducing the impact of ROCK-II could retard invadopodia formation, thus reducing colon cancer invasion and potentially slowing colon cancer progression.

Sensing tissue rigidity by touch has long been a primary indicator of abnormal tissue growth. It is known that cancerous tissues have a greater tissue density and rigidity than normal tissue. Increased density comes from two variables: an increase in cell density and an increase in ECM density. So it is important to understand the impact of these factors on cancer progression and whether these effects can be attenuated. Cells seeded at a higher density invaded further than those seeded at a lower density. However, when ROCK-I was inhibited, cells seeded at the lower density invaded much further than any of the other conditions. Similarly, ROCK-I knockdown led to increased invasion in low collagen density (1.5 mg/ml) and high density (4.0 mg/ml) scaffolds. The most significant impact of increasing collagen density was on cell proliferation,

where a 2-fold increase was observed. However, inhibiting ROCK-I attenuated the effect of increasing the collagen concentration on cell proliferation. While inhibiting ROCK-I may reduce the impact of dense environments on cell proliferation, it also causes the cell to lose its anchorage to the ECM by reducing its capacity to form focal adhesions.

Combining these results, ROCK-I and ROCK-II have differing impacts on colon cancer cell invasion within our three-dimensional model. Our collagen-rich model provides many sites for cell attachment, which causes cells to bind strongly to the scaffold. A reduction in the cells' ability to form focal adhesion due to reduced ROCK-I expression results in a loss of anchorage to the ECM. In our model, that loss increases cell invasiveness. While ROCK-I promotes cell-ECM interactions, ROCK-II disrupts cell-cell interaction. Consequently, this promotes epithelial to mesenchymal transition (EMT). By reducing ROCK-II expression, we were able to reduce the phenotype associated with EMT and consequently, were able to reduce colon cancer invasion in a 3D collagen I scaffold.

The results of this study are important to further understanding cancer. Other studies vaguely link ROCK to cancer invasion. This study showed that ROCK-I impacts cell invasion by impacting cell-ECM invasion and that ROCK-II impacts invasion by promoting the EMT phenotype. In the future, clinicians may be able to better control cancer progression by manipulating ROCK.

1.0 Introduction

Cancer remains one of the leading causes of mortality world-wide with colon cancer being the third most commonly diagnosed cancer and the third leading cause of cancer death in both men and women in the US (Jemal *et al.*, 2011; Siegel *et al.*, 2011). The American Cancer Society estimates 102,900 new cases of colon and 39,670 new cases of rectal cancer for 2010 and expected to cause 51,370 deaths (American Cancer Society, 2010). The incidence and mortality rates are especially high in African American populations. The risk of acquiring colon cancer greatly increases with age; most colon cancers are observed in patients who are greater than 50. Most younger patients who acquire colon cancer have a hereditary link (Strate and Syngal, 2005).

Patients who have polyps (benign abnormal growths) in the colon are at added risk of developing colon cancer. Patients who have had other conditions such as Inflammatory Bowel Disease (IBD) or even other cancers are at a greater risk at developing colon cancer (DeCosse *et al.*, 1994). In addition, diet plays an important role in colon cancer. For example, red meat consumption has been linked with a greater risk of colon cancer (Chao *et al.*, 2005). Extensive alcohol use has also been linked to increased colon cancer risk (Cho *et al.*, 2004; Mizoue *et al.*, 2006).

Anatomy

The large intestine is a major organ of the digestive tract. It is approximately five feet in length and can be up to three inches in diameter. All material not absorbed in the stomach and small intestines travels through the large intestines to be discarded as fecal matter. The initial portion is the Cecum. The majority of the large intestine is the colon. The terminal portion of the large intestine consists of the rectum and anus. The colon consists of four major portions: Ascending Colon, Transverse Colon, Descending Colon, and Sigmoid Colon. A figure illustrating the anatomy is shown in Figure 1.

The wall of the colon can be divided into five major layers (in order from inside to out): mucosa, submucosa, colonic muscle, subserosa, and serosa. The muscosa is the innermost tissue layer of the colon composed of epithelial cells, a thin layer of smooth muscle, and a layer of connective tissue called the lamina propria. Surrounding the mucosa is a layer of connective tissue called the submucosa. Next is the muscularis propria which is composed of circular and longitudinal smooth muscle. Surrounding this muscle layer is another layer of connective tissue called the subserosa. And finally, the outermost layer is a thin membrane layer composed of epithelial cells. This is illustrated in Figure 2.

Colon Cancer Formation

Cancer can be described as irregular and uncontrolled growth in a tissue or organ in the body. Colon cancer, as the name suggests, describes this growth with respect to the region of the colon. The cancer usually originates in the

mucosal layer and penetrates into the colon as the disease progresses. The general term used to describe the irregular tissue is a tumor. However not all tumors are cancerous.

It is not uncommon to have irregular growths which are not cancerous. These are called benign tumors. Common types of benign tumors are polyps and cysts. In fact, they account for the majority of irregular growths found. These growths are especially common amongst the older population. Most polyps in the colon are removed during colonoscopy.

While most polyps are benign, some could be either malignant or pre-malignant. These precancerous polyps, referred to as adenomas, are likely to evolve into malignancies if left untreated.

Diagnosis and Treatments

The predominant method in which colon cancers are usually discovered is through colonoscopy. The procedure involves inserting a long, thin, and flexible tube inside the patient's anus. The tube is composed of fiber optics which allow the healthcare practitioner to visualize the inner wall of the colon for any abnormalities. Presence of abnormalities such as polyps are often removed during the time of the procedure and taken for biopsy.

The most common method of treatment of colon cancer involves surgery. Depending on the severity of the cancer, this can result in removal of tumor or removal of portions of the colon itself. The most common (and least severe) form

of this is removal of a polyp during the time of colonscopy. In addition to colonoscopy, chemotherapy is also a common treatment. For higher grade tumors, chemotherapy is given to decrease the risk of recurrence and metastasis.

Classifying Colon Cancer

According to American Joint Committee on Cancer (AJCC), cancers are classified in different stages 0, I, II, III, and IV in increasing order of severity. Stage 0 represents tumors which are at the initial site and have not spread to any layers within the tissue. Stage I cancers which have invaded into the superficial layers of the tissue. Stage II describes cancers that have invaded deeper into the organ but has not spread to lymph nodes or distant tissues. Stage III represents increasing tumor size and possible spreading to regional areas such as lymph nodes. Stage IV cancers represent cells that metastasize or spread to other distant tissues and organs. Patients diagnosed with stage I cancer have low mortality rates while those diagnosed with stage IV cancer have poor survival rates.

These broad stages are based on a more intricate system known as the TNM system. As the name suggest, tumors are classified by three parameters as represented by the letters “T”, “N”, and “M” followed by a number. The first letter, “T”, represents the size of the primary tumor where the degree is measured numerically from 1-4, in increasing order of severity. The second

letter, “N”, represents the extent of spreading to regional lymph nodes where the degree is measured numerically from 1-3, in increasing order of severity. The third letter, “M”, represents the presence of metastasis to distant regions in the body. The presence of metastasis is denoted by a “1” and an absence of metastasis is denoted by a “0” (AJCC, 2002). This is shown in Table 1.

Colon cancer was originally staged by the Dukes’ staging system, developed by pathologist Cuthbert E. Dukes in 1932. There were four stages in this system: A, B, C, and D where these stages correspond closely with stages 1-4 for cancers. Stage A describes tumor invasion into the colon. Stage B describes tumor invasion deeper into the colon and possibly involving regional tissues but not involving lymph nodes. Stage C describes tumor invading into regional lymph nodes. Finally, Stage D describes tumor metastasis into distant regions of the body (Dukes, 1932).

A modified and more specific version was developed by Astler and Coller in 1954 (Astler and Coller, 1954). In this system, Stages B and C each have two substages 1 and 2. This modified version is very similar to the modern staging system. Stages B1 and B2 correspond to stages II-A and II-B, respectively, of the modern system. Similarly, stages C1 and C2 correspond to stages III-A and III-B, respectively, of the modern system. This system takes only the presence, not the extent, of nodal involvement in determining the stage.

Tumor Grading

According to the AJCC, tumors are graded in increasing order of severity from G1-4. Typically, the greater the numerical value of the tumor grade, the greater the progression of cancer. Lower-graded tumors are more differentiated. For epithelial cells, for example, more differentiated cells would exhibit a phenotype similar to epithelial cells. At the same time, less differentiated cells would not exhibit the characteristics of the native tissues. Poorly-differentiated and undifferentiated cells exhibit phenotypes closer to stem cells than what would be seen in the proper native tissue. This is summarized in Table 2.

Epithelial to Mesenchymal Transition

Colon cancers mostly start in the inner epithelial layer of the colon and migrate into the organ. Cancers with an epithelial origin are carcinomas and the vast majority of colon cancer belong to this category. It is important to understand how cells go from having a static, epithelial phenotype to an invasive, malignant phenotype. One possibility is through a process called epithelial-mesenchymal transition (EMT).

EMT describes a mechanism where epithelial tissue starts to develop characteristics more similar to stem cells. EMT is characterized by the loss of cell-cell adhesions (i.e. decreased E-cadherin expression) and increased cell motility. These cell-cell adhesions allow epithelial cells to act as a part of an entire unit, making epithelial tissue. Mesenchymal stem cells (MSC) behave in a

more independent manner. The goal of MSCs and other stem cells is to have the ability to different into various cell types which can form a variety of tissue layers. EMT is illustrated in Figure 3.

Various factors can induce EMT in cells. Some of these factors include matrix-metalloproteinases (MMP), secreted enzymes which have the ability to degrade collagen. For example, overexpression of MMP-9 has been shown to stimulate EMT in A431-III cells (Lin *et al.*; Lin *et al.*, 2011). Another study has shown that MMP-9 can induce EMT in renal tubular cells (Tan *et al.*, 2010). MMP-2 (Radisky and Radisky, 2010) and MMP-3 (Przybylo and Radisky, 2007) have also been linked to EMT. MMP-2, also known as gelatinase A, is a 72 kDa protein (Kerkela and Saarialho-Kere, 2003) which belongs to a larger family of matrix metalloproteinases, many of which have also been linked to cancer (McConkey *et al.*, 2009; Nannuru *et al.*, 2010; Szarvas *et al.*, 2011) .

Extracellular matrix components have also been linked to increased invasion. For example, type I collagen has been shown to induce EMT and down-regulates E-cadherin (Cheng and Leung, 2011). Other extracellular matrix components such as hyaluronic acid (HA) (Chow *et al.*, 2010) and fibronectin (Camara and Jarai, 2010) and have been linked to EMT. In addition to ECM, growth factors such as TGF-β (Yao *et al.*, 2004; Doerner and Zuraw, 2009; Zhang *et al.*, 2009), BMP-2 (Kang *et al.*, 2010), and VEGF (Chung *et al.*, 2011) have been shown to induce EMT.

Cell Adhesion

Different cell types need to be in the appropriate environment for survival and growth. Cells from tissues such as epithelial tissue require significant adhesion to either other cells or the extracellular matrix (ECM). This is where it is important to distinguish between studying cell behavior and studying tissue behavior. And since loss of cell adhesion contributes to cancer progression, it is also relevant in understanding cancer.

Cells in tissues such as epithelial tissues are bound to each other by cell junctions. There are three main classifications for cell junctions: communicating (gap) junctions, occluding junctions, and anchoring junctions. The most common type of communicating junction is the gap junction which allows molecules to pass freely through the cells. A common type of occluding junction is a tight junction which hold cells together and create a seal or barrier which prevent outside molecules from entering the intercellular space. Anchoring junctions, such as adherens junctions bind the cells together through adhesion molecules such as cadherins. These molecules attach to the actin cytoskeleton, assembling a cytoskeletal structure between cells of the same tissue (Alberts, 2002).

The predominant way by which cells attach to the ECM is through focal adhesions. In this situation, a receptor on the cell surface, called an integrin, binds to the ECM and is connected to the cell actin cytoskeleton through connection with proteins such as talin and vinculin. Integrins are heterodimers

consisting of an alpha and beta subunit. The beta subunit of the integrin binds to adaptor proteins such as talin and vinculin, which are bound to an actin filament inside the cell (Alberts, 2002). Outside the cell, the integrin attaches to specific amino acid sequence expressed on ECM molecules such as the RGD sequence found on laminin and fibronectin or DGEA found on type I collagen.

Rho-Kinase

Rho-kinase (ROCK) is a serine/threonine kinase involved with stress fiber formation and focal adhesions. There are two major isoforms of ROCK: ROCK-I and ROCK-II. Both isoforms are approximately 160 kDa in size and are 65% genetically identical with 92% identity in the kinase domain (Nakagawa, O. *et al.*, 1996). The reason behind having two isoforms or the variation between the isoforms is not completely clear.

ROCK is a downstream effector of RhoA. In this cascade, a signal is triggered by guanine exchange factors (GEFs), which promotes conversion of Rho-GDP to Rho-GTP. This activates ROCK which then activates LIM kinase and then cofilin which is involved with actin stablization (Kiss *et al.*, 1997). ROCK also induces stress fiber and focal adhesion formation by phosphorylating myosin light chain (MLC) (Leung *et al.*, 1996). The effect of ROCK activation affects both cell shape and motility. This is illustrated in Figure 4.

Despite the sequence similarities between ROCK-I and ROCK-II, it is important to observe them differently. In some cases, their physiological

functions are not identical and these differences could be vital to cell function and survival. Though no substantial differences in function have been observed between the two isoforms, ROCK-I and ROCK-II, these are activated by different mechanisms (Riento and Ridley, 2003). For example, ROCK-I but not ROCK-II has been linked to apoptosis, a term for programmed cell death. Specifically, ROCK-I is cleaved by Caspase-3 during apoptosis which leads to membrane blebbing (Coleman *et al.*, 2001; Sebbagh *et al.*, 2001). The cleaving eliminates the inhibitory domain and results in a 130 kDa fragment which is continuously active.

ROCK has been linked to metastasis in cancer. For example, ROCK has been linked to brain (Nakabayashi and Shimizu, 2011), bladder (Kamai *et al.*, 2003), ovarian (Jeong *et al.*, 2012), testicular (Kamai *et al.*, 2004) and lung cancer (Li *et al.*, 2006). For some cancers, the predominant isoform expressed varies. For example, ROCK-I expression was correlated with poorer outcomes for breast cancer patients (Lane *et al.*, 2008). ROCK-I has also been linked to metastasis in prostate cancer (Bu *et al.*, 2011). On the other hand, ROCK-II has been linked to metastasis in pancreatic cancer (Ivanov *et al.*, 2009). This shows that ROCK has been linked to metastasis in several forms of cancer and targeting it may be a useful form of treatment.

ROCK Inhibition

The most promising aspect of using ROCK inhibitors is applicability. Many compounds are able to affect cancer but never make it to a clinical trial. The ROCK inhibitor fasudil has been used in clinical trials in Japan since 1995 (Olson, 2008) and has been shown to be safe during clinical trials for cardiovascular disease (Suzuki *et al.*, 2007). Other ROCK inhibitors are being investigated for clinical applications. With the promise shown in the laboratory, could this be translated to the bedside.

There are several ROCK inhibitors that are commercially available. The most common ones in literature are H-1077 (fasudil), Fasudil is not specific for either ROCK isoform having a K_i value (binding affinity) of 0.4 μM (Liao *et al.*, 2007). Y-27632 is a more powerful ROCK inhibitor having K_i values of 0.22 μM and 0.3 μM for ROCK-I and ROCK-II, respectively (Ishizaki *et al.*, 2000). And H-1152 is the most potent of these inhibitors with a K_i value of 6 nM for ROCK-I and IC_{50} of 12 nM for ROCK-II (Liao *et al.*, 2007).

A recent study by Deng et al showed the effectiveness of using fasudil to suppress glioblastoma (GBM) progression. Treatment with the ROCK inhibitor fasudil reduced proliferation, migration, invasion, and matrix metalloproteinase-2 (MMP-2) expression (Deng *et al.*, 2010). According to this study, the effect of fasudil on GBM was dose dependent. When measuring cell migration, a low dose (5 μM) did not significantly affect migration with respect to the control. However, this result was different for higher doses. Treatment with 20 μM of

inhibitor resulted in a 30% reduction while treatment with 100 μM resulted in a 50% reduction of GBM cell migration.

In the same study, treatment with low dose fasudil did lead to lower invasion. Treatment with 5 μM led to a 40% reduction while treatment with 20 μM led to a 50% reduction in GBM invasion. Treatment with 100 μM of inhibitor led to a 70% reduction in invasion, confirming that fasudil can greater inhibit invasion by increasing the dose.

Treatment with medium and high doses of fasudil led to significant reductions in MMP-2 (matrix metalloproteinase-2) expression levels. This is important because MMP-2 expression has been linked to several forms of cancer (Jezierska and Motyl, 2009; Kenny and Lengyel, 2009; Libra *et al.*, 2009). In addition to suppressing protease-dependent forms of cell invasion, ROCK inhibition can also be effective in reducing the mobility of cells migrating in a protease-independent manner (Sahai and Marshall, 2003).

In addition to suppressing glioblastoma progression, fasudil has shown to reduce invasion in other cancers such as ovarian (Ogata *et al.*, 2009), lung (Ying *et al.*, 2006; Yang *et al.*, 2010), and breast (Ying *et al.*, 2006) cancers. This shows the potential of fasudil in decreasing tumor progression in all forms of cancer.

In addition to fasudil, other ROCK inhibitors have shown promise in the laboratory setting. In the paper by Deng et al, GBM cells were treated with 20 μM of another ROCK inhibitor named Y-27632. Treatment with this inhibitor also

showed significant reduction in migration, invasion, and MMP-2 expression in these cell lines. Treatment with the ROCK inhibitor Y-27632 has been shown to increase adhesion and reduce mobility of esophageal cancer cells (Wang *et al.*). Another study has shown that treatment with Y-27632 reduced MMP-2 and MMP-9 expression (Chang *et al.*, 2010).

In addition to its potential in treating cancer, ROCK inhibitors have shown promise treating cardiovascular disease (Tawara and Shimokawa, 2007) as well as various neurological disorders (Mueller *et al.*, 2005). The fact that these inhibitors have been thoroughly studied in other diseases also increases its applicability in a clinical setting.

Cancer in 3D

Why is it important to study cancer in a three dimensional setting? For years, research involving cancer cells dealt with plating cells on a planar surface (2D) and observing the biochemical reactions. Using these *in vitro* assays, we were able to test various drugs and their ability to affect cancer cells. Specifically, these drugs affected cancer cells through affecting their cell cycle. A common chemotherapy agent for colon cancer, 5-Fluorouracil, affects DNA synthesis, eventually leading to cell death. Another common chemotherapy drug (not for colon cancer), Paclitaxel also affects the cell cycle. Instead of altering nucleotide synthesis, this drug affects the cytoskeleton by stabilizing microtubules, impeding depolymerization (Jordan, 2002).

Conducting *in vitro* research at the two-dimensional level has given us valuable methods of treating the uncontrolled growth aspect of cancer. However, it has given clinicians very few tools for treating or predicting metastasis. The process by which cells break off from a primary tumor and migrate to a secondary location has as much to do with the physical environment as it does with the chemical one. Therefore, to understand metastasis, we must be able to recreate the tissue environment. One aspect of this environment is that it is not along a flat surface, but in three dimensions.

Studying cancer cells in three dimensions allows cells to interact with its environment providing a more realistic assessment. It provides depth, which gives the viewer an added dimension in both the visual experience and also in terms of understanding. An article by Alison Abbott (Abbott, 2003) emphasizes the point that studying biology in three dimensions is becoming more relevant. The applications vary from tissue engineering to studying cancer. Even cell culture techniques could be dramatically improved with the perspective of the added dimension. However, with all its benefits, imaging cells within a three-dimensional setting continues to be a limiting factor towards it becoming more widespread. Continued development of imaging techniques such as confocal microscopy and mulitphoton microscopy have made imaging in the added dimension more plausible.

Tissue Density

The concept of studying tissue density with respect to cancer has been around for ages. A healthcare practitioner uses palpations to access the qualitative texture and rigidity of a given tissue. Tissue which is stiff or irregular often indicates the risk of a potential malignancy. Medical imaging and eventually biopsies would be conducted to verify the presence of a malignancy.

Qualitative analysis of tissue density is also an important tool for analyzing tissue images. For example, mammography uses X-rays to view any potential malignancies. Areas of increased tissue density are considered a warning sign of a potential malignancy (Boyd *et al.*, 2009; Boyd *et al.*, 2010; Brower, 2010) in breast cancer. This means that those who have thicker breasts may be more susceptible for developing breast cancer.

Even though tumors have long been associated with irregular and stiff tissues, these factors have been greatly overlooked when studying cancer in terms of a scientific subject. Tissues consist of both cells and ECM. Most cancer related research has focused around the cellular and molecular aspects of tissues. Therefore, it is important to conduct cancer research which takes into account not only cellular and molecular aspects, but structural aspects of tissues as well.

2.0 RATIONALE

Colon cancer cells are surrounded by other cells and components when they invade in the body. In order to create an environment which more closely resembles the physiological environment, we seeded colon cancer cells onto 3D collagen scaffolds. By studying this in a 3D model, we would better understand how ROCK affects colon cancer invasion. **By inhibiting ROCK, we hypothesize that we can reduce the environmental impact on cancer cells, thus reducing their capacity for invasion**. In order to test this hypothesis, we will address the following aims.

2.1 Aim 1: Impact of ROCK on Colon Cancer

ROCK-II has been linked with greater invasion in several solid tumors (Horiuchi *et al.*, 2003; Kamai *et al.*, 2003). Studies performed in colon cancer cell lines have shown that over-expression of ROCK-II promotes tumor growth by reducing the association between tumor cells. This reduction in cell-cell adhesion promotes movement and allows for migration of endothelial cells into the tumor, a process that may lead to the formation of new vascular channels (Croft *et al.*, 2004). Furthermore, when ROCK-II is activated in *in vitro* colon cancer cell models it produced greater instability at the sites of adherens junction formation (Sahai and Marshall, 2002). While these studies have provided important information about the contribution of ROCK-II to the disruption of adherens

junctions in colon cancer, they do not fully answer the question of how it contributes to invasion in colon cancer.

In colon cancer, activity at the invasion front or advancing edge of the tumor has been demonstrated to be most predictive of further invasion and metastasis (Wood *et al.*, 1981; Hase *et al.*, 1993; Bosman, 1995). Since the major extracellular matrix component near the advancing edge of colon cancers is type I collagen (Pyke *et al.*, 1995), we examined the contribution of ROCK-II to colon cancer cell invasion at the tumor advancing edge using three dimensional type I collagen scaffolds and multiphoton microscopy in non-malignant and malignant colon cancer cell lines.

2.2 Aim 2: Impact of Cell Density on Colon Cancer

Using imaging techniques has also proved to be a useful tool in cancer diagnosis. In mammography, areas of increased tissue density are considered a warning sign of a potential malignancy (Boyd *et al.*, 2009; Boyd *et al.*, 2010; Brower, 2010). With this strong link between tissue density and cancer, there has not been sufficient *in vitro* studies conducted to understand this phenomenon. Furthermore, it is not certain if this is specific to breast cancer or more general to various forms of cancer, such as colon cancer.

Two variables involved with tissue density are cell density and extracellular matrix (ECM) density. From tissue engineering literature, we can observe the importance of cell-seeding density on overall cell fate. A study

(McBeath *et al.*, 2004) showed that initial seeding density played a greater role in cell differentiation than growth factors. Cells which are seeded in a denser environment exert greater mechanical stresses on other cells, which affect cytoskeletal arrangement through RhoA and eventually, Rho-kinase. Cell density has also been shown to be relevant in studying cancer. Using a colon cancer cell line, colon 26, it has been shown that metastasis is significantly greater in higher cell density environments (Kuwano *et al.*, 2004).

2.3 Aim 3: Impact of ECM Density on Colon Cancer

In addition to cell density, increased density of tumor tissue could also be attributed to an increased ECM density. Increased stiffness is also another result of increased collagen density. By using imaging techinques such as ultrasound, it has been shown that tissue stiffness can be quantified (Yen *et al.*, 2011).

Experiments proposed in the previous two aims are performed in 1.5 mg/ml scaffolds. However, tumor tissue typically has a rigidity consistent with collagen I concentrations greater than 2 mg/ml (Paszek *et al.*, 2005). So while this study is significant, it does not address how aggressive colon cancer cells would be affected by ROCK in more rigid environments which would be more consistent with tumor tissue. Therefore, it is vital to understand the impact of increasing collagen density with respect to ROCK and colon cancer.

3.0 Methods

Cell Lines: A total of three colonic cells lines were used in these experiments. NCM460 cells represent a non-malignant human colonic epithelial cell line (Moyer *et al.*, 1996) and were obtained from InCell, Inc (San Antonio, TX). Caco-2 E cells are a subclone of Caco-2 BBE cells and were obtained through a generous gift from Dr. Jerrold Turner at the University of Chicago. Caco-2 E cells are a non-aggressive colon cancer cell line derived from a tumor of unknown differentiation that appear villous on TEM. In contrast, SW620 cells are highly aggressive colon cancer cell line which was derived from a lymph node metastasis (Leibovitz *et al.*, 1976). They have been shown to produce liver metastases in nude mice (Flatmark *et al.*, 2004). SW620 cells were obtained from ATCC (ATCC# CCL-227).

***Cell Culture*:** NCM 460 cells were cultured in M3F Base supplemented with 10% fetal bovine serum (Gemini Bio-products) and were incubated at 37^{o}C in a 5% CO_2 atmosphere. Caco-2 E cells were cultured in D-MEM/F-12 (Mediatech) 50/50 1X with L-glutamine and 15mM HEPES supplemented with 10% fetal bovine serum and were incubated at 37^{o}C in a 5% CO_2 atmosphere. SW620 cells were cultured in Leibovitz's L-15 medium 1X (Mediatech) with L-glutamine supplemented with 10% fetal bovine serum and were incubated at 37^{o}C in a 1% CO_2 atmosphere.

Western Blotting: Cells were grown to confluence overnight. The next day, media was removed and cells were washed with ice cold PBS. A lysis buffer solution composed of 1:50 protease inhibitor cocktail in phosphate lysis buffer (PLB) was added to lyse the cell on ice. After 1 minute, cells were scraped off the surface and the contents were collected into a microfuge vial. The lysate were then subjected to 10 iterations of a freeze-thaw cycle. A freeze-thaw cycle entails submerging the lysates in a dry ice-ethanol solution for ten seconds followed by submerging the lysates in warm water for ten seconds. The vials were then centrifuged for 15 minutes at 10,000 rpm at 4 °C.

The next step involved equalizing protein concentrations between lysates. Protein concentration was analyzed using a BCA kit. 10 μl of sample or standard was added to each well. Then, a detection solution was created using two components. 200 μl of the detection solution was added to each well and the microplate was incubated at 37 °C for 30 minutes after which absorbance readings were taken at 550 nm. Using the standards, a line of best fit was created to correlate protein concentration based on absorbance readings.

For western blotting, we used 7.5% tris-HCl polyacrylamide gels (BioRad). 8 μl of dye was added to 40 μl of each sample. The dye consists of a 1:20 ratio of mercaptoethanol in Laemeli sample buffer. The dye-sample mixture was then heated for 8 minutes at 99 °C. Contents were then added to each well of the gel, saving the first lane for the marker. The gel was then submerged in a running buffer (tris, glycine, SDS) and the gel was run for 90 minutes. Initially, the voltage

was set to 80 V. After the samples completely invaded into the gel, the voltage was increased to 100 V.

Afterward running, the contents of the gel were to be transferred to a polyvinylidene fluoride (PVDF) membrane (Millipore). A transfer buffer solution (tris and glycine) was created with 20% methanol. Membrane was soaked in methanol before being placed on top of gel. Transferring was done for 1 hour at 100 V. Ice packets were placed next to the apparatus in order to keep the transfer buffer cool.

The gel was placed in a 5% milk solution (in TBST) to act as a blocking solution for 1 hour. Afterwards, the gel was washed with TBST and incubated with the appropriate primary antibody overnight. ROCK-II was at 1:100 and Actin was at 1:100 as well. The following day, the gel was washed again with TBST every 5 minutes, repeated 3 times. ROCK-II (1:5,000) and Actin (1:5,000) HRP-labeled secondary antibodies were added for 1 hour and washed again with TBST.

Antibodies were detected on the membrane by being exposed to a solution made from an ECL kit (GE Healthcare). Components from each of the two bottles were mixed in equal quantities. The solution was then placed on the membrane, covering the entire area of the membrane for 2 minutes. The membrane was then dipped in water and placed face-down onto plastic wrap. Film was placed on top of the membrane in a dark room and then placed into a developer.

***Creation of 3-D scaffolds*:** Three-dimensional (3D) cell cultures will be performed as previously described(Sun *et al.*, 2004). Briefly, 3 mg/ml type 1 collagen (BD) in 0.1 M acetic acid was mixed with equal portions of 0.1 M NaOH, 0.7% sodium bicarbonate, and Hank's Balanced Salt solution for a final type 1 collagen concentration of 1.5 mg/ml. The pH was adjusted to 7.4 and serum free culture media was added so that it made up 30% of the mixture. Predetermined amounts of this mixture were placed on glass supports and allowed to gelatinize. A low density of the colonic epithelial cell line of interest (200,000 cells/cm^2) was then be plated on top of the gel. Gels were incubated at 37°C for 1 hr. at which time an additional 2 ml of appropriate media was added.

Immunocytochemistry: Cell-containing collagen scaffolds were cultured for up to 5 days in a 37°C CO_2 incubator. Scaffolds were then be washed with phosphate buffered saline (PBS), fixed overnight in 10% neutral buffered formalin (NBF). Collagen scaffolds were then washed and permeabilized with tris buffered saline with 0.05% Tween-20 (TBST) for 15 minutes. After this, the scaffolds were blocked for 20 minutes with serum free protein block (Dakocytomation) and then washed again with TBST. After washing, scaffolds were incubated overnight at 4°C with desired primary antibody. Scaffolds were then washed with TBST the following day and then incubated with a fluorescently labeled (FITC or TRITC) secondary antibody for one hour. Scaffolds were then washed with PBS and incubated in a 1:20 phalloidin dye (for F-actin staining) for

30 minutes. Scaffolds were then washed again with PBS and then water (Note: important to wash with water prior to DAPI staining). Finally, the scaffolds were incubated in a 1:1000 DAPI solution for 5 minutes. For best results, scaffolds were then kept in PBS at 4 °C overnight prior to imaging.

Multiphoton Microscopy: Collagen fibrillar structure and seeded cells were imaged by a laser scanning multiphoton confocal microscope with 60x oil objective (NA=1.40). DAPI was visualized by using multiphoton laser excitation at 700 nm and emmision at 450 nm, for which the femosecond laser beam (80MHz, 0.5mW) pumped from a mode-locked titanium:Sapphire laser (MaiTai, Spectra-Physics Inc., CA), was coupled with visible laser (Bio-Rad, UK) into an inverted laser scanning confocal microscope (Nikon TE200-U, Japan). Reflection signals from the collagen fibers were excited and acquired at a wavelength of 488 nm.

Transmission Electron Microscopy: Cells were plated on top of type 1 collagen scaffolds as above and allowed to invade over a 24 our period. At the end of this time, the media was removed, the scaffolds were washed with sterile PBS, and then fixed with 3% gluteraldehyde in 0.1 M sodium cacodylate buffer. Post fixation, the cell-containing scaffolds were treated with 1% osmium tetrachloride and dehydrated using graded ethanol. The samples were then infiltrated with and embedded in epoxy resin, LX112 (Ladd). 83 nm sections were made a Leica Ultracut II and placed on 150 mesh nickel grids. Sections

were then steamed for 20 min. in a citrate based antigen retrieval solution (DakoCytomation). When cool, the sections were then blocked using serum free protein block (DakoCytomation). Each section was then probed for the primary antibody of interest for 2 hours followed by the appropriate biotinylated secondary antibody for 1 hour. Finally, sections were incubated with strepavidin-gold (6 nm gold particle) at 1:20 dilution in TBS, pH 7.6 for 1 hour and then counterstained with 5% uranyl acetate and Reynold's lead citrate. Sections were viewed and images were obtained using a JEOL JEM-1220 transmission electron microscope. Primary antibody concentrations used were as follows: cortactin, MMP-2, 9, and 13 were used at 10 mg/ml, ROCK-II was used at 20 mg/ml.

Proliferation Assay: Cell proliferation was determined using a standard MTT assay kit. All components used were free of phenol red, since it may have interfered with the accuracy of the assay. To do this, the media was removed from each chamber and the gels were washed with PBS. When removing the media or the PBS, it is important to avoid disrupting the scaffold as much as possible. 100 μL fresh media and 20 μL of dye ((3-(4,5-dimethylthiazol-2-yl)-2,5-diphenyltetrazolium bromide) in PBS was added to each well. The gels were incubated at 37 °C for four hours. After four hours, 50 μL from each chamber was added to 100μL of dimethyl sulfoxide (DMSO) in a small vial and incubated for ten minutes. Absorbance readings were taken at 550 nm for each sample to determine the cell proliferation values.

ROCK siRNA: Short interfering RNA (siRNA) is a short sequence (20-25 nucleotides in length) which has the ability to inhibit the expression of a specific gene. It binds to the mRNA, making it ineffective. The gene cannot be translated; therefore, it cannot be expressed.

All siRNA experiments were performed in environments free of RNAase. In order to ensure this, the area and equipment were treated with an RNAase remover. NCM460, Caco-2 E, and SW620 cells were plated at a density of 200,000 cells/cm^2 overnight. The following day, media was removed and cells were washed with PBS. The siRNA transfection itself had three conditions: ROCK-II knockdown, scrambled, and an untransfected condition. ROCK-II knockdown represents silencing the expression of ROCK-II. Scrambled represents using a mock siRNA sequence which does not knockdown a specific gene. Added 10 μl of ROCK-II or scrambled siRNA (Santa Cruz Biotechnology) to 200 μl of transfection medium (Santa Cruz Biotechnology). Transfection medium alone was used for the untransfected condition.

Next, 30 μl of transfection reagent (Santa Cruz Biotechnology) was added to 600 μl of transfection medium. Soon afterwards, 210 μl of this mixture was added to each of the three conditions and incubated at room temperature for 30 minutes. Before adding these mixtures to the cells, the cells were washed with tranfection medium. After washing, 200 μl of the transfection mixure and 800 μl of transfection medium was added to each well and allowed to incubate for 6 hours. After 6 hours, cell-line specific media supplemented with 20% FBS was

added to each well and then incubated. All volumes presented were on a per well basis. Transfection efficiency was determined by western blot approximately 48 hours post transfection.

Matrix Metalloproteinase Assay: MMP-2,9, and 13 levels were quantitatively assessed using a colorimetric ELISA (R&D Systems). The microplate came precoated with either a polyclonal (MMP-2) or a monoclonal (MMP-9,13) antibody. 100 μl of assay diluent was added to each well and then 50 μl of each standard or sample was added to each well. This was incubated at room temperature for 2 hours on a horizonal orbital shaker (Eppendorf) at 500 rpm. After two hours, the contents were removed from each well and each well was washed 4 times with a wash buffer. Next, 200 μl of conjugate (enzyme conjugated antibody) to each well for 4 hours at room temperature at 500 rpm. After 2 hours, wash the wells again 4 times. Next, add 200 μl of substrate solution to each well for 30 minutes. The substrate solution activates the enzyme bound to the antibody which produces a bluish color with the intensity dependent on the amount of bound antibody. After 30 minutes, add a stop solution to stop the reaction taking place. Upon adding this solution, the contents in the wells should turn yellow. Then a dual absorbance reading at 450/570 nm was taken using a microplate reader (BioRad).

***Cell Density Scaffolds*:** SW620 cell were plated at seeding densities of 50,000 and 250,000 cells/cm^2 overnight. 6-well and 24-well plates were used to create the affect of different seeding densities without altering the total number of cells in each scaffold. Type I collagen hydrogels were constructed using a high concentration (8-11 mg/ml) type I rat tail collagen (BD Biosciences) in 0.1 M acetic acid. Gels were created according to the instructions provided by the manufacturer. First, a predetermined amount (10% of final volume) of cold PBS 10X was placed into a vial. Next the volume of collagen to be added was calculated using the following equation:

$$\frac{V_c = V_f \times C_f}{C_s}$$

Where V_c represents the volume of collagen to be added, V_f represents the volume of the final mixture, C_f represents the final concentration of the collagen mixture, and C_s represents the concentration of the rat tail collagen I bottle provided by the manufacturer. C_f in this case is 1.5 mg/ml Next, 0.023 × V_c of 1 M NaOH was added to the vial with PBS 10X. Then cold media was added to this vial. The amount of media to be added was calculated using the following formula:

$$V_m = 0.9\ V_f - 0.977\ V_c$$

Finally, the predetermined amount of collagen was added to the vial and gently mixed to create a homogenous solution. It was important to keep this mixture

cool before adding it to the wells to prevent any unwanted gelation. Gels were incubated at 37°C for 1 hr. at which time an additional 2 ml of appropriate media was added.

Boyden Chamber Assay: Initial cell invasion was analyzed using a commercially available colorimetric invasion assay purchased from Millipore (Billerica, MA). The assay consists of inserts with 8 µm pore polycarbonate membrane precoated with collagen. The inserts were soaked with 300 µL of warm serum-free media for 30 minutes at room temperature in order to rehydrate the collagen coating. After this incubation, 250 µL of media was carefully removed from the inserts. Next, SW620 cell suspensions were created and added to the inserts in order to give seeding densities of 50,000 or 250,000 cells/cm2 in each well. Serum-free media was added to the insert to obtain a final volume of 250 µL in the upper chamber. Next, 500 µL of serum supplemented with 10% FBS was added to the bottom chamber, making sure the membrane has full contact with the media in the lower chamber.

The wells were then incubated at 37 °C for 72 hours in a CO2 free incubator. After 3 days, media was removed and the insert containing the membrane were placed in wells containing 400 µL of a cell stain for 20 minutes at room temperature. The inserts were wash in water and noninvading cells were removed from the top portion of the insert using a clean cotton swab. The inserts were then placed in 200 µL of an extraction buffer for 20 minutes at room

temperature. 100 μL of this solution was placed into each each of a 96-well microplate reading and an absorbance reading was taken at 550 nm.

Imaging With Cell Tracker: Cell-containing collagen scaffolds were cultured for up to 5 days in a 37°C incubator (no CO_2). Scaffolds were then be washed with phosphate buffered saline (PBS), fixed overnight with 10% neutral buffered formalin (NBF), and then permeabilized with tris buffered saline with 0.05% Tween-20 (TBST) for 15 minutes. After this, the scaffolds were blocked for 20 minutes with serum free protein block and then washed with TBST. Scaffolds were labeled with 10 μM of a CellTracker Orange CMTMR dye for 30 minutes and then washed with PBS.

Seeded cells were imaged by a laser scanning multiphoton confocal microscope with 40x objective (NA=1.40). Cells labeled with the CellTracker dye were visualized by using multiphoton laser excitation at 541 nm and emission at 565 nm, for which the femosecond laser beam (80MHz, 0.5mW) pumped from a mode-locked titanium:Sapphire laser (MaiTai, Spectra-Physics Inc., CA), was coupled with visible laser (Bio-Rad, UK) into an inverted laser scanning confocal microscope (Nikon TE200-U, Japan).

Invasion Depth: A series of stacked images of different planes were taken using a multiphoton microscope. The number of stacks viewed was based on the presence of cells. The combination of the stacks was rotated 90 degrees to

provide a side view (where 0 degrees would be a top view). Cell distance from the glass surface was measured at various points. The system was calibrated to present the depth in microns.

ROCK Activity: Seeded SW620 cells were seeded on top of 1.5 mg/ml collagen I gels. In order to reach the desired seeding density, seeded cells onto scaffolds in 6-well (50,000 cells/cm^2) and 24-well (250,000 cells/cm^2) plates. Cells were treated with Y-27632, a common ROCK inhibitor and the untreated condition was used as the control.

ROCK activity was analyzed using an ELISA kit (Cyclex). Briefly, 10 μl of the appropriate sample or standard was added to each precoated well. Next, 90 μl of a kinase reaction buffer (kinase buffer and ATP) was added to each well. This was incubated for 30 minutes at 30°C. Each well was washed five times with a wash buffer. Next, each well was incubated with an HRP conjugated antibody for 1 hour at room temperature. The wells were again washed five times. After washing, each well was treated with 100 μl of a substrate solution for ten minutes to detect the presence of antibody. This turns the contents of the wells blue. Finally, 100 μl of a stop solution was added which turned the contents of the well yellow. A dual absorbance measurement was taken at 450/550 nm using a standard microplate reader (BioRad).

***Collagen Density Scaffolds*:** SW620 cells were plated at a seeding density of 250,000 cells/cm^2 on each well overnight. The following day, cells were washed with PBS. Collagen I gels of either 1.5 or 4.0 mg/ml were placed on top of the cells, allowing the cells to invade into the gels.

Type I collagen hydrogels were constructed using a high concentration (8-11 mg/ml) type I rat tail collagen (BD Biosciences) in 0.1 M acetic acid. Gels were created according to the instructions provided by the manufacturer. First, a predetermined amount (10% of final volume) of cold PBS 10X was placed into a vial. Next the volume of collagen to be added was calculated using the following equation:

$$\frac{V_c = V_f \times C_f}{C_s}$$

Where V_c represents the volume of collagen to be added, V_f represents the volume of the final mixture, C_f represents the final concentration of the collagen mixture, and C_s represents the concentration of the rat tail collagen I bottle provided by the manufacturer. Next, $0.023 \times V_c$ of 1 M NaOH was added to the vial with PBS 10X. Then cold media was added to this vial. The amount of media to be added was calculated using the following formula:

$$V_m = 0.9\ V_f - 0.977\ V_c$$

Finally, the predetermined amount of collagen was added to the vial and gently mixed to create a homogenous solution. It was important to keep this mixture cool before adding it to the wells to prevent any unwanted gelation. The

scaffolds were incubated for 1 hour at 37 °C after which 2 ml of media was added to each well.

Statistics: Data was analyzed using Student's t distribution using average values and the associated standard deviation. A comparative p-value of less than 0.05 was considered significant.

4.0 Results

4.1 ROCK-II Impacts 3D Colon Cancer Invasion in Collagen I Scaffolds

ROCK-II Is Overexpressed in Colon Cancer Cells: To begin, it was necessary to establish a model system in which to evaluate ROCK-II's behavior. To do this, we first evaluated ROCK-I and II expression in non-malignant (NCM460) and malignant (Caco-2 E and SW620) colonic epithelial cell lines. This is shown in Figure 5. NCM460 cells are a non-malignant human colonic epithelial cell line (Moyer *et al.*, 1996). Caco-2 E cells are a non-aggressive colon cancer cell line derived from a tumor of unknown differentiation that appear villous on TEM. In contrast, SW620 cells are highly aggressive colon cancer cell line which was derived from a lymph node metastasis (Leibovitz *et al.*, 1976). They have been shown to produce liver metastases in nude mice (Flatmark *et al.*, 2004). Despite these differences in phenotype, all three cell lines expressed low levels of ROCK-I and both colon cancer cell lines over-expressed ROCK-II.

ROCK-II Localization Differs Between Non-Malignant and Malignant Colon Cancer Cells: Because intracellular localization often provides insight into function, we next evaluated ROCK-II expression of each colonic epithelial cell line in type I collagen scaffolds. Type I collagen was chosen because it is a predominant ECM protein in the advancing edge of colon cancers (Pyke *et al.*, 1995). The scaffolds were created to be fairly stiff so as to have a rigidity more reminiscent of the tumor microenvironment in at the advancing edge of a tumor.

As described in the Methods section, cells were seeded into a well and a 1.5 mg/ml collagen I gel was created on top of the cells where the cell were allowed to invade and remodel over up to three-day period. Figure 6 shows ROCK-II distribution at 24 hours post invasion. The red and green pseudocoloring represents actin and ROCK-II, respectively. Intriguingly, ROCK-II co-localized with the actin cytoskeleton in non-malignant cells (Figure 6A) shown by the presence of yellow spots. At the same time, NCM460 cells in these collagen scaffolds did not contribute to matrix degradation (Figure 7A). In sharp contrast, there were no signs of ROCK-II co-localizing with actin in either Caco- 2 E cells (Figure 6B) or SW620 cells (Figure 6C). ROCK-II localized to the periphery of the cell and did not co-localize with actin in any colon cancer cell line. Furthermore, significant degradation of the collagen matrix was noted adjacent to these collections (Figure 7B, 7C). Since ROCK-II expression in cancer cells is directional and adjacent to degraded collagen, this led us to hypothesize that these ROCK-II collections may actually be associated with a matrix degrading structure such as invadopodia.

Invadopodia are podosome-like structures capable of focal matrix degradation (Buccione *et al.*, 2004; Marx, 2006; Weaver, 2006; Yamaguchi *et al.*, 2006; Nagi and Bleiweiss, 2007). They were first identified in breast cancer cell lines and have classically been seen in an “invadopodia” assay wherein cells are seeded on fibronectin coated gelatin and the number of matrix degrading

extensions is noted. We used trasmission electron microscopy (TEM) in order to verify the presence of subcellular structure such as invadopodia.

ROCK-II Localizes to Invadopodia: To confirm that these structures were invadopodia, we plated each cell line at equal densities on type I collagen scaffolds and processed them for TEM as described in the Methods section. In non-malignant NCM460 cells, no structures representing invadopodia were noted. In Caco2-E and SW620 cells, structures resembling invadopodia were noted. Since SW620 cells had the greatest number and most prominent invadopodia-like structures, we probed them with antibodies to cortactin, ROCK-II, MMP-2, MMP-9, and MMP-13 (Figure 8). Biotinylated antibodies were bound to 6 nm gold nanoparticles conjugated to streptavidin. The presence of heavy metals such as gold appears black in TEM.

A projective structure extending from the cell body was observed (Figure 8A). The presence of cortactin was evaluated because this protein has been shown to be a marker of invadopodia (Bowden *et al.*, 1999; Artym *et al.*, 2006; Bowden *et al.*, 2006). The projective structures we observed in this highly invasive colon cancer cell line were positive for both cortactin and ROCK-II. Cortactin staining was present at the base of structures shown in Figure 8B. The presence of ROCK-II antibodies (Figure 8C) was far more significant and heavy ROCK-II expression was noted throughout the structure, validating the presence of invadopodia in the fluorescence pictures (Figures 6, 7).

To confirm that these projections possessed matrix degrading ability, we probed SW620 cell sections for several matrix metalloproteinases (MMPs) that have been previously localized to invadopodia, specifically MMP-2, MMP-9, and MMP-13. MMP-2 has been previously localized to invadopodia (Nagase, 1998) and action on MMP-2 by MMP-1 has been shown to lead to clustering of its active form at the site of invadopodia (Coopman *et al.*, 1998; Deryugina *et al.*, 2001). MMP-9 has been localized to invadopodia in highly invasive breast cancer cells (Bourguignon *et al.*, 1998) and MMP-13 has been previously shown to localized to invadopodia in several gastric cancer cell lines(Elnemr *et al.*, 2003).

Evaluation of each of these MMPs revealed localization to the sites of invadopodia. The most significant expression of MMP-2 was seen at the tip the invadopodia as shown in Figure 8D. The presence of MMP-9 at the tip was not as significant; there appeared to be a small spec of MMP-9 expressed at the tip, pointed to in Figure 8E. Expression of MMP-13 was the most significant of the three MMPs tested. Shown in Figure 8F, the tip of the invadopodia is saturated in black, indicating a strong presence of MMP-13. While all three MMPs were present, MMP-2 and MMP-13 were the most robust and clustered at the tips of the invadopodia along with ROCK-II. While this data confirmed that ROCK-II localized to invadopodia, it was critical to prove that it was a critical mediator of colon cancer cell invasion.

ROCK-II Mediates Colon Cancer Cell Invasion: To verify that ROCK-II mediated invasion via invadopodia in colon cancer cell lines, we next evaluated the effect of knocking down ROCK-II with siRNA on depth of invasion, MMP expression, and proliferation as described in the Methods section. All siRNA experiments were performed with a scrambled sequence siCONTROL, which did not significantly reduce ROCK-II expression, depth of invasion, proliferation, or MMP expression. Transfection efficiency of ROCK-II siRNA in all cell lines was between 60-90% and transfection of a scrambled sequence of siCONTROL did not suppress ROCK-II expression (Figure 9).

The most significant contribution of ROCK-II knockdown was seen in SW620 cells. Untransfected SW620 cells had an average invasion of approximately 90 microns while those transfected with ROCK-II siRNA had an average invasion of 44 microns (Figure 10). This indicates that ROCK-II knockdown decreased SW620 cell invasion by half. There was no significant decrease due to ROCK-II knockdown in either NCM460 or Caco-2 E cells. This data suggests that ROCK-II knockdown reduces invasion in the most aggressive colonic cancer cell line.

A visual representation of the difference in invasion between untransfected (Panels A, C) and those transfected with ROCK-II siRNA (Panels B, D) is shown in Figure 11. In addition to the decreased invasion depth due to ROCK-II knockdown, it is also important to note the morphological changes due to

silencing ROCK-II expression. ROCK-II knockdown resulted in SW620 obtaining a significantly rounder morphology (Figure 11B, 11D) compared to untransfected SW620 cells (Figure 11A, 11C). Furthermore, ROCK-II knockdown appeared to significantly decrease the actin signal.

ROCK-II Mediates Proliferation in Normal Cells, not Malignant Cells: It could be hypothesized that less invasion occurred because siRNA inhibition of ROCK-II impaired cell proliferation. The data, however, suggests that this is not the case. NCM460, Caco-2 E, and SW620 cells were seeded and transfected with ROCK-II siRNA for 48-72 hours where the untransfected condition served as the control. The proliferation values of cells within type I collagen scaffolds were obtained as described in the Methods section. When proliferation was evaluated in the absence and presence of ROCK-II siRNA, approximately 50% decrease in proliferation was observed in non-malignant NCM460 cells but no significant change in proliferation was observed in either Caco-2 or SW620 colon cancer cell lines (Figure 12).

ROCK-II Influences MMP Expression: Using multiphoton microscopy and TEM, it has been demonstrated visually that ROCK-II localizes to invadopodia in colon cancer cells along with MMP-2, 9, and 13. Since ROCK-II is expressed at the site of invadopodia, we hypothesize that it could be involved with the expression of matrix-degrading proteins. Suggesting this, we evaluated MMP-2, 9, and 13 expression using commercially available sandwich ELISA kits. The

experiments were carried out as described in the Methods section. All cell lines were subjected to siRNA and were in type I collagen scaffolds. We had previously observed MMP-2 expression at the tip of invadopodia on TEM. ROCK-II knockdown reduced MMP-2 expression in both the colonic cancer cell lines (Caco-2E and SW620) but had no significant impact on non-malignant colonocytes (NCM460). This data is shown in Figure 13.

On TEM, there was some though inconsistent presence of MMP-9 in invadopodia. When all three cell lines were transfected with ROCK-II siRNA, there appeared to be no significant impact on MMP-9 expression (Figure 14). On the other hand, there was a significant expression of MMP-13 on the tip of the invadopodia displayed on the TEM image. Similar to its effect on MMP-2 expression, ROCK-II knockdown reduced MMP-13 expression in malignant cells (Caco-2 E and SW620) but had no significant impact on non-malignant cells (NCM460). This data is shown in Figure 15. To summarize, knockdown of ROCK-II led to significant reduction (P=0.05) in both MMP-2 and MMP-13 in both colon cancer cell lines but not in non-malignant cells.

4.2 ROCK-I Inhibition Increases 3D Invasion at Low Seeding Densities

Cell Seeding Density Affects Characteristics in 3D: Cell seeding density is an important aspect of tissue structure. In order to understand how cell density affects cancer tissue, SW620 cells were seeded at 50,000 and 250,000 cells/cm^2 onto 1.5 mg/ml collagen I gels and incubated at 37 °C for a period of five days. Scaffolds were treated with 10 μM of the ROCK inhibitor Y27632 added daily to the scaffolds. No treatment with ROCK inhibitor was used as the control condition. Cells were stained with phalloidin and imaged using a multiphoton microscope.

Cells seeded at the lower cell density appeared to have relatively few cell-cell interactions. Within the collagen scaffold, these cells exhibited a symmetrically round phenotype. There were protrusions or invadopodia as observed in prior experiments using SW620 cells (Vishnubhotla *et al.*, 2007). Cells seeded at the higher density were tightly packed within the 3D scaffold. This resulted in a forced contact between the cells which resulted in an inconsistent cell morphology. It is important to note that the cells which appear rounder are on a plane above the rest of the cells. This can be seen in Figure 16.

Increased Cell Density Leads to an Increase in ROCK Activity: Since cells seeded at a higher density have a greater likelihood of interacting with one another, it was important to address whether this impacts ROCK activity. ROCK

activity was assessed using a commercially available ELISA kit. SW620 cells were seeded at 50,000 and 250,000 cells/cm^2 onto 1.5 mg/ml collagen I gels and incubated at 37 °C for a period of five days. Scaffolds were treated with 10 μM of the ROCK inhibitor Y27632 added daily to the scaffolds. No treatment with ROCK inhibitor was used as the control condition. The cells were lysed and the contents were collected and protein concentrations were equalized.

ROCK activity was significantly increased due to an increase in cell density. Scaffolds with cells seeded at 250,000 cells/cm^2 had ROCK activity that was more than double that of cells seeded at 50,000 cells/cm^2. It is important to note that cell density was altered by changing the seeding area and not the number of cells seeded. The results are shown in Figure 17.

Treatment with Y-27632 Decreases Invasion in Boyden Chambers: A common method of quantitatively assessing the cell invasion is by using Boyden chambers. Therefore, SW620 cells were seeded at 50,000 and 250,000 cells/cm^2 onto the inside of Boyden chambers and allowed to invade through over 72 hours at 37 °C. Chambers were treated with 10 μM of the ROCK inhibitor Y27632 added daily to the scaffolds. No treatment with ROCK inhibitor was used as the control condition.

Cells seeded at a higher density did have more cells invade than those seeded at a lower density. It should be noted, however, that the initial number of cells was also greater for the higher density, thus making this comparison

irrelevant. The result which was most significant was that ROCK inhibition with Y-27632 decreased in invasion in higher cell densities while it had minimal impact on invasion at lower seeding densities. The results are shown in Figure 18.

Treatment with Y-27632 Increases Invasion at Low Densities: While Boyden chambers are an effective model in measuring the initial point of invasion, they do not adequately assess how cells move through bulk tissue. Therefore, invasion must be measured in an environment which more closely resembles native tissue. To achieve this, SW620 cells were seeded at 50,000 and 250,000 cells/cm^2 onto 1.5 mg/ml collagen I gels and incubated at 37 °C for a period of five days. Scaffolds were treated with 10 μM of the ROCK inhibitor Y27632 added daily to the scaffolds. No treatment with ROCK inhibitor was used as the control condition.

Samples were tracked using a cell tracker dye. Seeding density did affect invasion depth of SW620 cells in collagen I scaffolds. Cells seeded at 250,000 cells/cm^2 invaded twice the distance than those seeded at 50,000 cells/cm^2 for untreated. However, this effect was not observed for SW620 cells treated with Y-27632. For cells seeded at the lower seeding density, treatment with Y-27632 led to a 3.5-fold increase in invasion depth. However, no significant increase was observed in cells seeded at 250,000 cells/cm^2. This is graphed in Figure 19.

Increasing Cell Seeding Density Increases Proliferation: While altering cell density and inhibiting ROCK impact invasion, it is still unclear how these factors influence another relevant factor for cancer tissue: proliferation. To understand this, SW620 cells were seeded at 50,000 and 250,000 cells/cm^2 and incubated at 37 °C for a period of five days. Scaffolds were treated with 10 μM of ROCK inhibitor Y27632 with inhibitor added daily to the scaffolds. No treatment with ROCK inhibitor was used as the control condition. Cell density was altered by changing the area while keeping the overall number of cells constant.

Cell seeding density impacted cell proliferation. Increasing the cell seeding density from 50,000 cells/cm^2 to 250,000 cells/cm^2 led to a 2.5-fold increase in proliferation for untreated cells. For cells treated with Y27632, increasing cell seeding density led to a 1.5 increase in proliferation.

For cells seeded at 50,000 cells/cm^2, treatment with Y-27632 led to a 1.5 fold increase in cell proliferation compared to that of the untreated samples. However, for cells seeded at 250,000 cells/cm^2, treatment with the ROCK inhibitor did not appear to have a significant impact on cell proliferation. This data is shown in Figure 20.

4.3 Silencing ROCK-I Increases Invasion in Both Collagen Densities

ROCK-I Knockdown Leads to Increased Invasion: In order to better understand cancer at a tissue level, it is important understand the interaction of cancer cell with their environment influences the outcome. SW620 cells were transfected with siRNA to knockdown ROCK-I where untransfected cells were used as the control. After transfection, the cells were seeded onto collagen I gels of concentrations of 1.5 and 4.0 mg/ml and incubated at 37 °C for a period of three days. Samples were tracked using a cell tracker dye.

Increasing collagen concentration did seem to reduce overall invasion, though the effect was slight. Cells seeded onto 4.0 mg/ml collagen I gels had approximately 20% decrease in invasion depth to those seeded onto 1.5 mg/ml gels for both ROCK-I knockdown as well as untransfected cells. For both 1.5 and 4.0 mg/ml collagen I gels, ROCK-I knockdown resulted in a 1.6-fold increase in invasion depth compared to untransfected cells. This data is shown in Figure 21.

Dense Collagen Gels Increase Proliferation: While collagen concentration alone had a minimal affect on invasion, ROCK-I knockdown increased invasion. Next, it is important to observe whether these trends translate over to cell proliferation. To do this, SW620 cells were transfected with siRNA to knockdown ROCK-I where untransfected cells were used as the control. After transfection, the cells were seeded onto collagen I gels of concentrations of 1.5 and 4.0 mg/ml and incubated at 37 °C for a period of three days.

Collagen concentration had a significant impact on proliferation of untransfected SW620 cells. Cells seeded onto 4 mg/ml collagen gel had a proliferation value which was 2.5 fold greater than that seen in cells seeded onto 1.5 mg/ml collagen gels. However, cells where ROCK-I was knocked down resulted in a 1.3 fold increase by increasing collagen concentration.

There was no significant difference between ROCK-I knockdown and ROCK-II knockdown with respect to cell proliferation in either of the collagen concentrations. However, the impact of ROCK knockdown varied with different collagen concentrations. ROCK-I knockdown led to an insignificant decrease in cell proliferation in 1.5 mg/ml gels. However, for cells in collagen gels of 4.0 mg/ml, proliferation decreased by 50% due to ROCK knockdown. This data is shown in Figure 22.

5.0 DISCUSSION

Cancer remains one of the leading causes of mortality world-wide with colon cancer being the third most commonly diagnosed cancer and the third leading cause of cancer death in both men and women in the US (Jemal *et al.*, 2011; Siegel *et al.*, 2011). ROCK has been felt to be a possible target in this battle against metastatic disease but its role in invasion has not been well understood. Because ROCK-II has been linked with greater invasion and metastasis in several solid tumors, we evaluated ROCK-II's contribution to colon cancer cell invasion in dense type I collagen scaffolds-an environment more reminiscent of the advancing edge of colon cancer.

What are the mechanisms behind tumor cell invasion? One mechanism is forming structures which aid in cell motility such as podosomes and invadopodia. These structures are actin–rich cellular protrusions which aid a cell's motility. Podosomes are commonly found in normal cells such as leukocytes, endothelial cells, smooth muscle cells, and osteoclasts while invadopodia are typically observed exclusively in malignant cells (Linder, 2007). In addition, podosomes tend to be much smaller, in greater number, and occur for a shorter duration than invadopodia. In addition, invadopodia have the capacity to degrade the surrounding ECM by secreting proteases (Weaver, 2006). This capacity to eliminate surrounding matrix to aids cancer cell motility.

Since invadopodia have matrix-degrading ability, it is important to assess the impact of ROCK-II on matrix-degrading protein secretion. Our data confirms

the finding by others that ROCK is involved in the activation of matrix metalloproteinases, specifically MMP-2, MMP-9, and MMP-13 (Fukushima *et al.*, 2005; Meriane *et al.*, 2006). Furthermore, it identifies ROCK-II as the critical isoform of ROCK involved in activation of both MMP-2 and MMP-13. MMP-9 activity has also been linked to Rho/ROCK (Turner *et al.*, 2005), but our data did not show a significant decrease in MMP-9 activity with ROCK-II knockdown. At the same time, MMP-9 expression on TEM was not as robust as those of MMP-2 and MMP-13. The reason for this is not clear but what is clear is that there is regulation of MMPs by ROCK-II in the setting of an *in vitro* colon cancer model. Furthermore, the link between MMP-13 and ROCK-II in colon cancer confirms the retrospective studies that associated MMP-13 with a poor prognosis in colon cancer (Leeman *et al.*, 2002; Klinge *et al.*, 2006) as well as the studies showing that inhibition of ROCK not MMPs attenuates invasion (Wyckoff *et al.*, 2006).

The finding of ROCK-II co-localizing with invadopodia was not expected particularly in light of the recent literature showing ROCK to be a mediator of amoeboid cell movement (Torka *et al.*, 2006; Wyckoff *et al.*, 2006; Sahai *et al.*, 2007). Mesenchymal cell movement is associated with matrix degradation whereas amoeboid cell movement relies on the cell's ability to use the force of actomysin to push collagen fibers out of the way. A study by Sahai et. al. reported that mesenchymal invasion by breast cancer, colon caner, melanoma, and fibrosarcoma cell lines is mediated by Smurf1 promotion of RhoA degradation and subsequent decrease in ROCK activity. Furthermore, this group

reported that when Smurf1 is inhibited, invasion increases and cell movement becomes more amoeboid due to an increase in ROCK activity. Intriguingly, the inhibitors used in this study targeted ROCK-I (Y-27632) (Tamura *et al.*, 2005) and did not target MMP-13 (Torka *et al.*, 2006; Wyckoff *et al.*, 2006). Similarly, two other groups have also linked ROCK with amoeboid cell movement. A study by Wyckoff et. al. reported that ROCK-I and ROCK-II both contribute to amoeboid cell movement. In this study, a highly invasive breast cancer cell line, MTLn3E, was studied in 4 mg/ml type I collagen gels. One could argue at this density that mesenchymal cell movement was not necessary because of the increase in porosity of the gel created by tight packing of collagen fibers (Torka *et al.*, 2006; Wyckoff *et al.*, 2006). A third paper by Torka et. al. reported that inhibition of ROCK with Y-27632 in aggressive breast cancer cells grown in 1.67 mg/ml type I collagen scaffolds led these cells to change from an amoeboid to a mesenchymal appearance (Torka *et al.*, 2006; Wyckoff *et al.*, 2006). We would argue that these results are due to the fact that the cells were grown on tissue culture plastic and not surrounded by a type I collagen matrix. Taken together, these studies confirm that ROCK-II may have different activities depending on chemical and mechanical signals of the local microenvironment (Wozniak *et al.*, 2003). In addition, they emphasize the importance of the tumor microenvironment to understanding and predicting tumor cell invasion. In the case of colon cancer invasion, our *in vitro* model shows that a colon cancer cell's ability to invade at

the tumor advancing edge is mediated, in large part, by the action of ROCK-II on MMP-2 and MMP-13 at the site of invadopodia.

It is interesting to observe the contrast between inhibiting ROCK-I and reducing ROCK-II expression via siRNA. It needed to be determined whether ROCK-I inhibition would yield similar results to ROCK-II siRNA in our 3D collagen model. We altered the cell seeding density in order to understand the effects that cell-cell interactions play in 3D cancer invasion. The most significant change in SW620 proliferation as a consequence of ROCK inhibition was seen in cells seeded at the lowest density. At this density, cells were spread out through the scaffold, with minimal cell-cell contact. It has been shown that cells do proliferate more in high cell-density environments (Pardee, 1989; Nelson and Chen, 2002). So, it is not surprising that cells seeded at the highest density have greater proliferation than those seeded at the lowest density.

The most surprising, yet revealing data comes from studying invasion depth of varying densities of SW620 cells in 3D collagen I scaffolds. Treatment with Y-27632, one of the most common ROCK inhibitors, resulted in an increase in SW620 cell invasion in some conditions. This was observed in the low cell density condition (50,000 cells/cm^2), where there were few cell-cell interactions. In the high cell density condition (250,000 cells/cm^2), there appeared to be an insignificant change due to ROCK inhibition. The vast difference in invasion profiles of the varying cell densities implies the importance of cell-cell interactions on cell invasion. However, the mechanism for this is not yet understood.

The difference in the impact of ROCK inhibition on invasion using boyden chambers and our 3D collagen I scaffold are significant. Boyden chambers are effective in modeling how a cancer cell would invade at the initial point of invasion into the basement membrane. However, this model is not relevant to later stages of cancer because it does not measure the extent of tumor invasion through tissues. A collagen I scaffold is more representative of how cancer cells move through tissue. The impact of ROCK inhibition could vary not only by cell type, but by its environment.

Other studies have shown that treatment with Y-27632 led to decreased metastasis. A study (Liu *et al.*, 2009) demonstrated that treatment with Y-27632 reduced invasion of breast cancer cells both *in vitro* and *in vivo*. It has been shown in another study that Y27632 decreased the expression of LIMC and MLC suggesting inhibition of metastasis (Kidera *et al.*, 2010). Furthermore, Y-27632 has also been shown to reduce invasion by reducing the attachment with the ECM in an *in-vivo* model of meningitis (Nakagawa, H. *et al.*, 2005). Treatment with these ROCK inhibitors, especially Y-27632, has also been shown to initiate loss of stress fibers and a concomitant decrease in tyrosine phosphorylation of paxillin and focal adhesion kinase (FAK) (Ramachandran *et al.*, 2011), thus reducing cell-ECM contact.

We have linked ROCK-II knockdown with lesser invasion by reducing the presence of invadopodia and protease secretion in SW620 cells (Vishnubhotla *et al.*, 2007). However, these studies used siRNA to knockdown ROCK-II and not

chemical inhibitors. So, it is important to understand the differences between ROCK-II knockdown via siRNA and using a ROCK inhibitor such as Y27632. One important difference is that Y27632 targets both isoforms of ROCK, ROCK-I and ROCK-II. In fact, Y27632 is a more potent inhibitor of ROCK-I than ROCK-II (Ishizaki *et al.*, 2000).

Is the discrepancy in cancer cell invasion due to differing affects of ROCK-I and ROCK-II? Though Y-27632 is a more potent inhibitor of ROCK-I, it still has some inhibitory effect on ROCK-II. Therefore, we wanted to observe the impact of silencing ROCK-I expression on cancer cell invasion and proliferation. For these set of experiments, we also observed the effects of ECM density. For the untransfected samples, the average invasion depth between the differing collagen concentrations is quite similar. However, upon looking at the data and the images more closely, invasion in these scaffolds are not identical with one another. The cells are more spread out in 1.5 mg/ml scaffolds than they are in 4.0 mg/ml scaffolds, represented numerically by a higher deviation.

Collagen concentration appears to have a significant impact on SW620 cell proliferation where proliferation increased 2.5-fold (Figure 22). A past study has shown the relative elastic modulus values based on collagen concentration where a 1.5 mg/ml collagen gel would be around 200 Pa and a 4.0 mg/ml gel would have an elastic modulus of approximately 1,600 Pa (Paszek *et al.*, 2005). This same study also showed that the increased stiffness increased colony size. One may question whether this is due to matrix stiffness or other factors. A study

(Schrader *et al.*, 2011) observed a dramatic increase in proliferation of hepatocellular carcinoma cells (HCC) when placed on a stiff environment. The same study also concluded that cells plated on a soft environment exhibited more stem cell characteristics. Another article made the argument that increasing matrix stiffness increases cell proliferation and differentiation (Wells, 2008), supporting the data shown in the previous study. All this taken together supports the concept that ECM stiffness plays a large role in colon cancer proliferation.

ROCK inhibition attenuated the effect of increasing collagen density. In this case, integrins binding to the collagen matrix activates the Rho/ROCK pathway. This in turn increases cellular contractility. In flexible or soft microenvironments, cells are able to contract the matrix easier which facilitates the formation of tubular structures. However, in stiff and rigid microenvironments, matrix contraction become more difficult which results in greater proliferation (Wozniak *et al.*, 2003). This could be linked to the crosstalk between the Rho and Ras pathways (Sahai *et al.*, 2001). Difficulty in contracting the matrix would impede the formation of the proper architecture and may promote excessive proliferation and disorganized architecture as seen in neoplastic growth (Huang and Ingber, 2005). Furthermore, increasing cell contractility in turn leads to ECM stiffening which creates a self-perpetuating cycle in which cells become more and more proliferative. This unregulated growth, or neoplasia could eventually lead to cancer. ROCK inhibition reduced the impact of the stiffer matrix and could be possible treatment option for uncontrolled growth.

While matrix stiffness had a significant impact on cancer cell proliferation, it had minimal impact on invasion. Furthermore, the impact of each ROCK isoform varies with respect to cancer cell invasion. Much of this could be related to how each isoform is involved with attachment. For example, ROCK-I has been linked to facilitate stress fiber formation and promote focal adhesions in fibroblasts (Yoneda *et al.*, 2005). In the same study, ROCK-II has been linked to increased phagocytotic uptake. Another study has shown that ROCK-I knockdown led to decreased adhesion while ROCK-II knockdown led to increased adhesion in keratinocytes on fibronectin (Lock and Hotchin, 2009). However, there is nothing to explain why the adhesions of the two isoforms with the ECM may differ.

The underlying question that needs to be addressed is: how do the two isoforms of ROCK contribute to cell-cell and cell-ECM interactions? The fact that ROCK-I is involved with focal adhesions (Yoneda *et al.*, 2005) means that it is directly correlated with cell-ECM interactions. ROCK-I inhibition would lead to fewer focal adhesions and thus, cells would have less attachment to the extracellular matrix. This decreased attachment would lead to cells having less anchorage. In ECM-rich environments, this loss of cell anchorage would allowing cells to move more freely, which makes them potentially more invasive.

Reduced focal adhesions could explain why SW620 cell invasion increased due to ROCK-I inhibition. These cells would lose their attachments to the ECM more easily, allowing them to migrate further. However, this does not

explain why ROCK-II knockdown had the opposite response to cell invasion compared to ROCK-I knockdown. Another study (Alvarez *et al.*, 2008) has shown that inhibiting ROCK-I expression reduced migration by limiting focal adhesions. However, there is no evidence that ROCK-II has an antagonistic relationship with ROCK-I with regards to focal adhesion formation.

A study has linked ROCK-II to disrupting apical junctions (Samarin *et al.*, 2007). Furthermore, this effect was linked to ROCK-II but not ROCK-I. A following study further linked this towards cancer cell dissociation and metastasis (Ivanov *et al.*, 2009). The involvement of ROCK-II in disrupting cell junctions reduces a tissue's capacity to form an epithelial phenotype. It may be this effect of ROCK-II which is most relevant for cancer progression and metastasis.

It is possible that ROCK-II is associated with both amoeboid and mesenchymal motility. Both forms of motility require actin at the site of invasion. Amoeboid movement requires actin to alter a cell's shape to allowing its penetration through tissue. Mesenchymal movement requires actin for the formation of matrix-degrading structures such as invadopodia. Though most present literature defines ROCK's role to amoeboid movement, it is likely that it is involved in both forms of motility. Furthermore, many studies (discussed previously) have linked ROCK inhibition to a more mesenchymal phenotype. The argument in many research articles is that ROCK is positively correlated to amoeboid motility and negatively correlated with mesenchymal motility.

The data presented in this project discounts the notion that ROCK is solely involved with amoeboid movement. This project has shown a significant amount of data which show that ROCK-II inhibition reduces the presence of invadopodia, decreases the amount of MMPs present, and decreases the overall invasion in metastatic cell lines. This data provides strong evidence that ROCK-II is involved with mesenchymal motility, especially in metastatic SW620 cells.

The fact that ROCK-II plays a role in disrupting cell-cell adhesion is of critical importance. A defining characteristic of epithelial mesenchymal transition (EMT) is the loss of cell adhesion. For cells which have undergone EMT, the loss of cell-cell contact enables them to be more motile. As shown in Figure 11, ROCK-II knockdown in SW620 cells caused the cells to lose a more mesenchymal phenotype, but also have the cells packed more regularly with each other, which would be consistent of a more epithelial phenotype. It has been shown that ROCK inhibition has shown to inhibit EMT in cardiac cells (Zhao and Rivkees, 2004). Considering its role in disrupting cell adhesion, it is not only plausible, but also likely that ROCK-II knockdown negated some of the effects of EMT and induced a more epithelial phenotype.

While ROCK-II effect on invasion seems to be related to cell-cell interactions and EMT, ROCK-I seems to have a greater effect on cell-ECM interactions. As mentioned earlier, ROCK-I has been shown to be involved with focal adhesion formation. By inhibiting ROCK-I, we are reducing the capacity for the cells to form attachments to the ECM. The effect of this on cell motility

depends on the surrounding environment. In studies performed on a two-dimensional substrate, reducing a cell's capacity to form focal adhesions would reduce its motility. However, since a collagen hydrogel contains numerous sites for attachment for any migrating cell, this reduced attachment caused an increase in invasion.

This theory also explains the results behind the SW620 cell density invasion data. In a low cell density environment, cells are spread apart. When treated with a ROCK inhibitor that targets both isoforms, invasion increased due to reduced cell-ECM attachment from ROCK-I inhibition. However, ROCK-II inhibition did not have a dramatic effect on reducing EMT because the cells were already apart. However, in a high density environment, ROCK inhibition did not appear to have a dramatic effect on invasion. Having a cluster of cells made it difficult for the cells to invade as readily as the low cell density condition. This is also seen in collagen concentration data. Here, ROCK-I knockdown led to an increased invasion due to a less significant anchorage to the ECM in both low and high density collagen scaffolds.

In summary, this study has show the impact of ROCK-I and ROCK-II on cancer cell invasion in 3D collagen I scaffolds. It also showed how reducing ROCK expression (both isoforms) negates the impact of a stiffer matrix on cancer cell proliferation. Further understanding of how ROCK impacts cancer could lead to future treatments which can allow clinicians to more effectively manage the disease.

6.0 CONCLUSION

6.1 Summary of Results

1. We have determined that ROCK-II is expressed at the leading edge of colon cancer. This has been observed both in histological staining of colon cancer specimens as well as in fluorescence microscopy of colon cancer cells lines within a 3D collagen I scaffold (1.5 mg/ml collagen).

2. Using fluorescence microscopy, ROCK-II expression is observed in NCM460, Caco-2 E, and SW620 cells. Its expression is diffused in the nonmalignant NCM460 cells. However in malignant cells, collections of ROCK-II are observed at the cell periphery. This is most apparent in SW620 cells where ROCK-II is expressed in extensions from the main cell body. Furthermore, the expression observed in malignant Caco-2 E and SW620 cells were adjacent to areas of degraded collagen.

3. We hypothesized that ROCK-II collections found along cell periphery and protrusions were involved with invadopodia. Invadopodia are protease secreting projections which aid cell invasion in malignant phenotypes. We confirmed the presence of these structures using TEM. On TEM, there was heavy ROCK-II expression was observed along the protrusion. Furthermore, matrix degrading proteases MMP-2 and MMP-13 were expressed at the tip of these protrusions, confirming that these structures are invadopodia.

4. ROCK-II expression was knocked down using siRNA. ROCK-II knockdown did not significantly impact invasion for NCM460 or Caco-2 E cells. However, silencing ROCK-II expression did significantly reduce the invasion of SW620 cells in 3D collagen I scaffolds. Furthermore, ROCK-II knockdown resulted in SW620 cells exhibiting fewer protrusions; which would imply ROCK-II knockdown led to a decreased presence of invadopodia in SW620 cells.

5. In order to validate ROCK-II's role in invadopodia, we knocked down ROCK-II expression and observed expression of various MMPs. ROCK-II knockdown did not significantly impact MMP expression in nonmalignant NCM460 cells. However, in malignant Caco-2 E and SW620 cells, ROCK-II knockdown led to a significant reduction in MMP-2 and MMP-13 expression. Considering that these two proteases were expressed at the tips of the invadopodia on TEM, we conclude that ROCK-II is involved in invadopodia in colon cancer cell lines.

6. ROCK-II impacts proliferation differently for nonmalignant and malignant phenotypes. In nonmalignant NCM460 cells, ROCK-II knockdown led to a reduction in cell proliferation. However in both malignant cell lines, ROCK-II knockdown had no significant impact on proliferation. This result shows that the reduced invasion of SW620 cell due to ROCK-II knockdown is not due to reduced cell proliferation.

7. Cells were plated at two separate seeding densities, one a low density where cells were spread out, and on a high density where cells were close to other cells. We observed the effect of treating both seeding condition with ROCK inhibitor Y27632 (which inhibits both isoforms). Treatment with this inhibitor resulted in a dramatic increase in invasion for cells seeded at a lower density but not in those seeded at a higher density. ROCK inhibition appears to have varying affects on invasion based on cell density. Also, ROCK-I and ROCK-II may have differing effects and mechanisms on cell migration.

8. ROCK-I knockdown led to a significant increase in invasion for SW620 cells. This was then observed in a higher collagen density scaffold (4 mg/ml), which led to a similar result. This confirms that ROCK-I and ROCK-II have different impacts on colon cancer invasion in our model.

9. Increasing the collagen scaffold density from 1.5 mg/ml to 4.0 mg/ml greatly increased proliferation (~3-fold increase). ROCK knockdown did not significantly impact proliferation in the lower density scaffold, but reduced proliferation by over 50% in the higher density scaffold. The proliferation values upon ROCK knockdown were similar to those observed in 1.5 mg/ml scaffolds. This suggests that ROCK knockdown reduces the impact of the physical environment on colon cancer cell proliferation.

ROCK-I and ROCK-II have different impacts on various cell processes which leads to different impacts of knockdown. ROCK-I is more involved with focal adhesions and other cell-ECM interactions. ROCK-II can disrupt cell-cell junctions and silencing ROCK-II may improve cell-cell adhesion. Furthermore, ROCK-II's role in disrupting cell-cell adhesion could make it a potential promoter of EMT. We have also observed that silencing ROCK-II expression not only reduces invasion in SW620 cells, but also promotes cells to exhibit a more epithelial phenotype. These cells had a consistent shape, had fewer protrusions, and were ultimately less invasive. These results are shown in Figure 23. Taken together, silencing ROCK-II expression may have the potential to reduce the impact of EMT.

6.2 Future Directions

While the data presented in this work demonstrated that ROCK-II is involved in invadopodia formation and colon cancer metastasis, more work has to be done to understand the underlying mechanisms for this phenomenon. Furthermore, data presented has shown that ROCK-I and ROCK-II have differing impacts on colon cancer invasion in a 3D collagen type I scaffold. In the Discussion section, the presented theories implied that ROCK-I and ROCK-II have different roles and impacts on cell adhesion where ROCK-I has a greater impact on cell-ECM adhesion while ROCK-II has a greater impact on disrupting cell-cell junctions. While evidence in literature may support this notion, there need to be further studies to test the validity of these claims.

Future set of experiments should be created with the goal of confirming the significance of each ROCK isoform on cell adhesion. It should be verified whether ROCK-II does disrupt cell-cell junctions, especially in poorly differentiated cells such as the SW620 cell line. At the same time, it should be observed if ROCK-I also plays a critical role in disrupting (or aiding) the formation of cell junctions. Similarly, the role and effect of ROCK-I and ROCK-II should be verified with respect to attachment to collagen substrates. These studies would need to be performed on both two as well as 3D substrates. It would be interesting to see if either of the two ROCK isoforms has a differing affect on attachment based on the dimensionality of the substrate.

Performing experiments on both two and 3D substrates could also offer other insights. Does the effect that ROCK has on cell morphology depend on the substrate? It is quite conceivable since cell geometry may be affected by the locations of its attachments. Since 2D substrates are planar, adhesion to these substrates will also be only along one plane. However, attachment to three-dimensional substrates would be from multiple directions. It would be interesting if ROCK inhibition led to one type of morphology on a two-dimensional substrate and a different morphology on a three-dimensional substrate.

Finally, it would be useful to create models correlating cell invasion to ROCK inhibitor concentration and collagen concentration. In order to do this, a greater number of concentrations have to be used compared to those used in this study. Being able to correlate these concentrations to invasion would more accurately describe the impact that ROCK inhibition and collagen density have on colon cancer invasion. Furthermore, it would reveal further the nature of the relationship between ROCK, collagen concentration, and colon cancer invasion.

APPENDIX A

TNM Stage	Tumor *Stage*	Observed in Colon Cancer
Tis N0 M0	Stage 0	Tis: Tumor located on site only in mucosa
T1 N0 M0	Stage I	T1: Tumor invades into submucosa
T2 N0 M0	Stage I	T2: Tumor invades into muscle layers
T3 N0 M0	Stage II-A	T3: Tumor invades into subserosa
T4 N0 M0	Stage II-B	T4: Tumor invades into adjacent regions
T1-2 N1 M0	Stage III-A	N1: Tumor spreads to 1-3 regional lymph nodes
T3-4 N1 M0	Stage III-B	N1: Tumor spreads to 1-3 regional lymph nodes
T1-4, N2, M0	Stage III-C	N2: Tumor spreads to > 4 regional lymph nodes
T1-4, N1-4, M1	Stage IV	M1: Tumor spreads to other regions in the body

Table 1: Correlating TNM staging system to numerical stage and description of each stage. (AJCC 2002)

Tumor Grade	Differentiation
G1	Cells are well-differentiated
G2	Cells are moderately-differentiated
G3	Cells are poorly-differentiated
G4	Cells are undifferentiated

Table 2: Correlating tumor grade to level of cell differentiation (AJCC 2002). Increased grading indicates increased cancer progression.

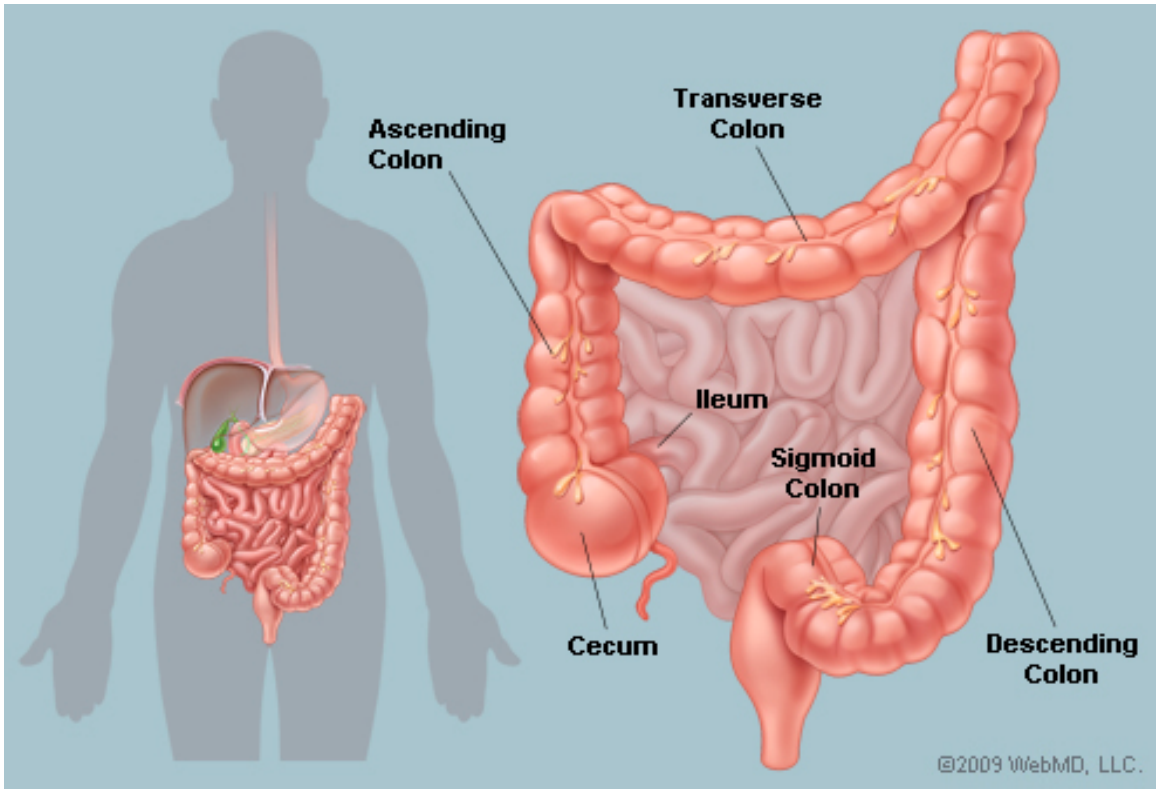

Figure 1: Image describing the anatomy of the colon shown above (Copyright ©2009, (WebMD), LLC. All rights reserved)

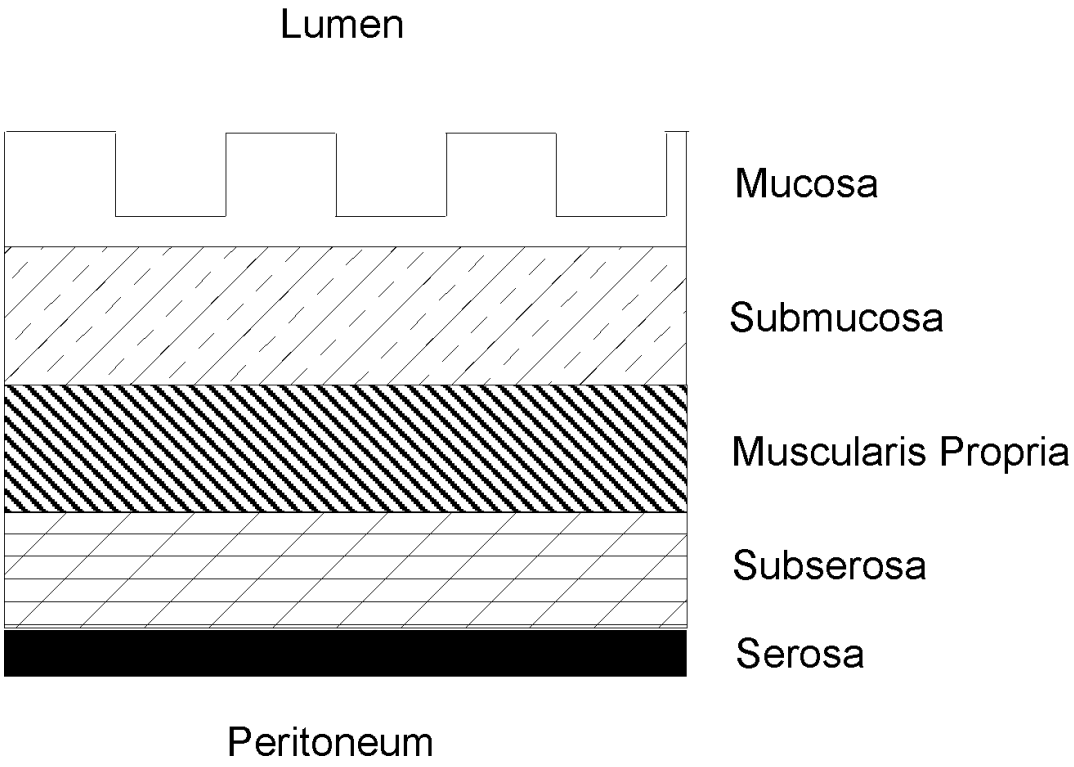

Figure 2: Figure representing the tissue layers inside the human colon.

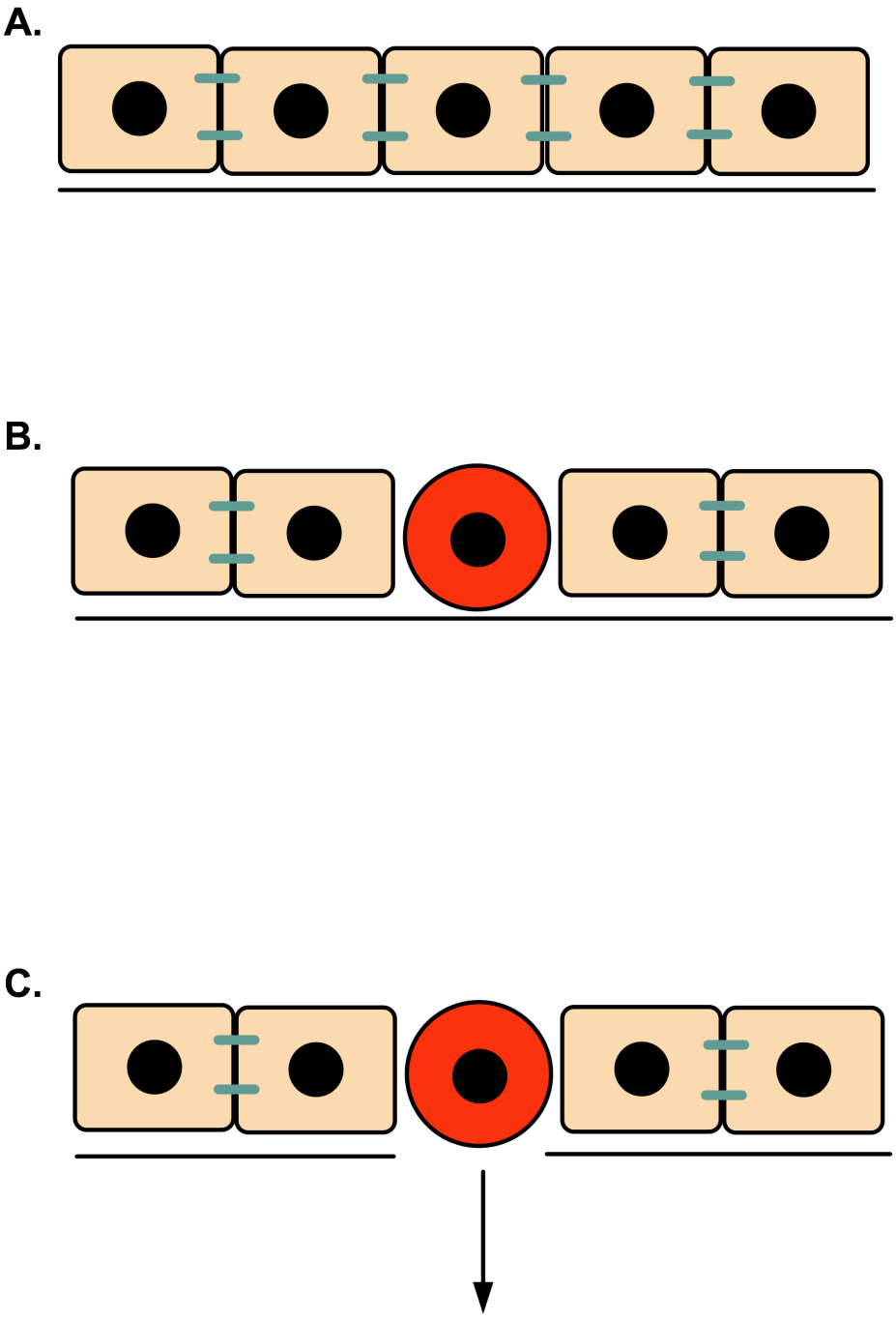

Figure 3: Figure illustrating epithelial-to-mesenchymal transition (EMT). Cells are arranged uniformly in the epithelial state (A). Upon EMT, cell-cell junctions are disrupted (B). Cells that have undergone EMT are more motile and can invade tissues (C).

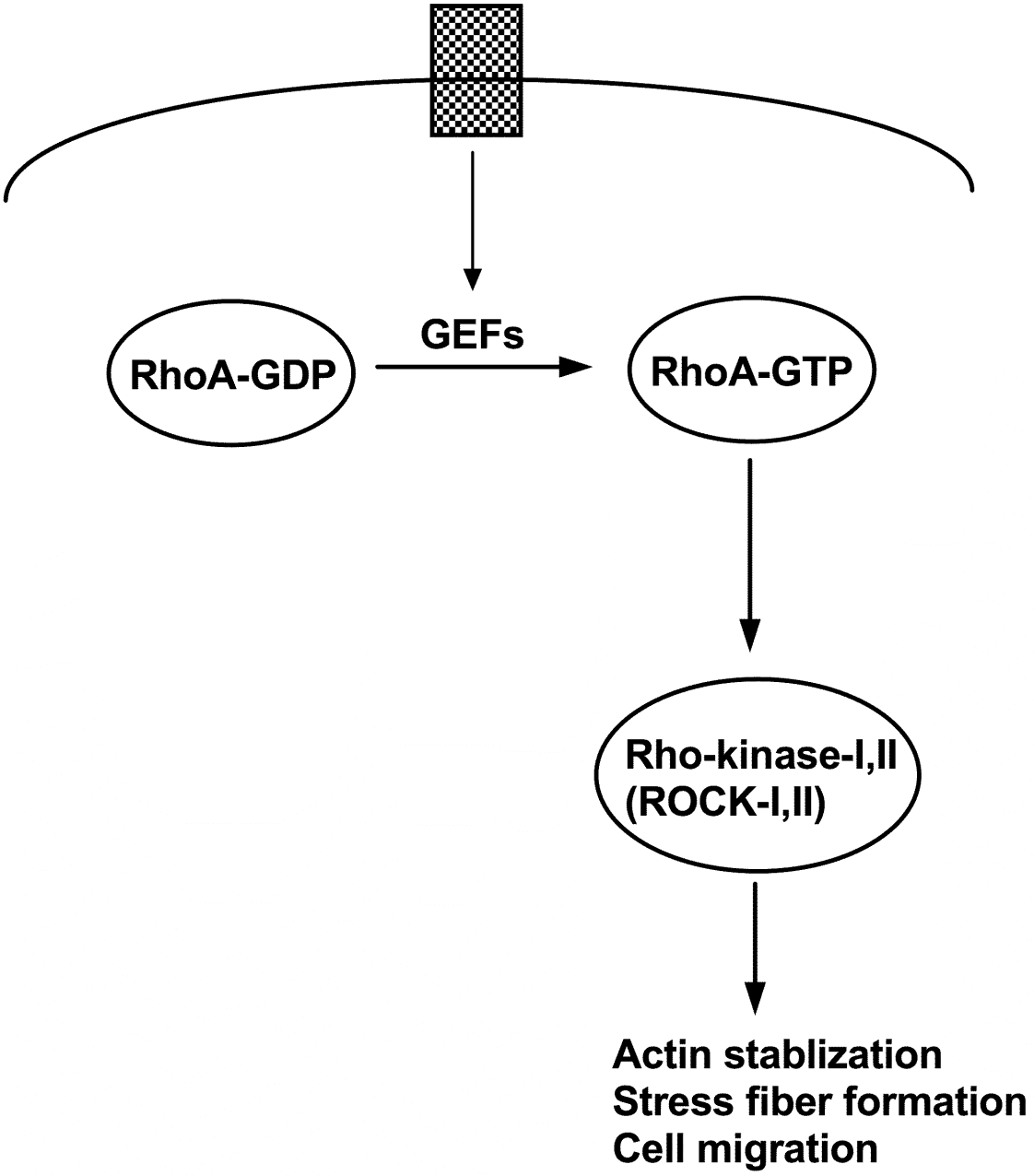

Figure 4: Diagram illustrating the RhoA/ROCK pathway. Rho GEFs assist RhoA exchange GDP for GTP. This activates ROCK which promotes actin stabilization, stress fiber formation, and cell migration.

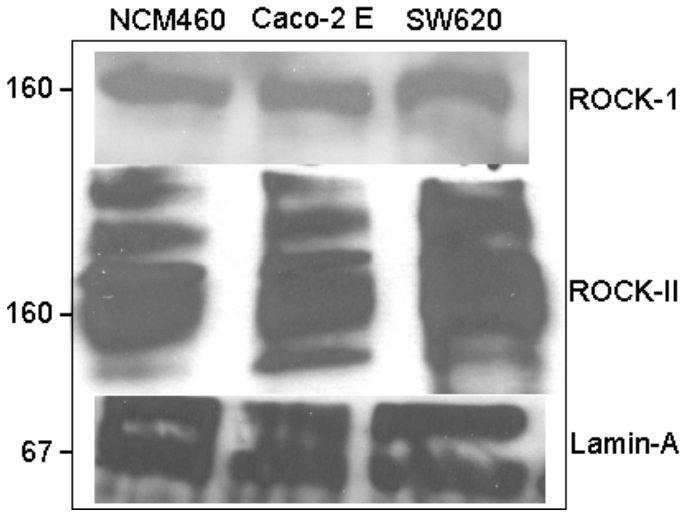

Figure 5: Western blot illustrating low ROCK-1 (upper panel) and high ROCK-II (middle panel) in both non-malignant and malignant colonic epithelial cell lines studied. There is greater ROCK-II expression in the malignant cell lines as compared with the non-malignant cell line. Lamin-A was used as a loading control.

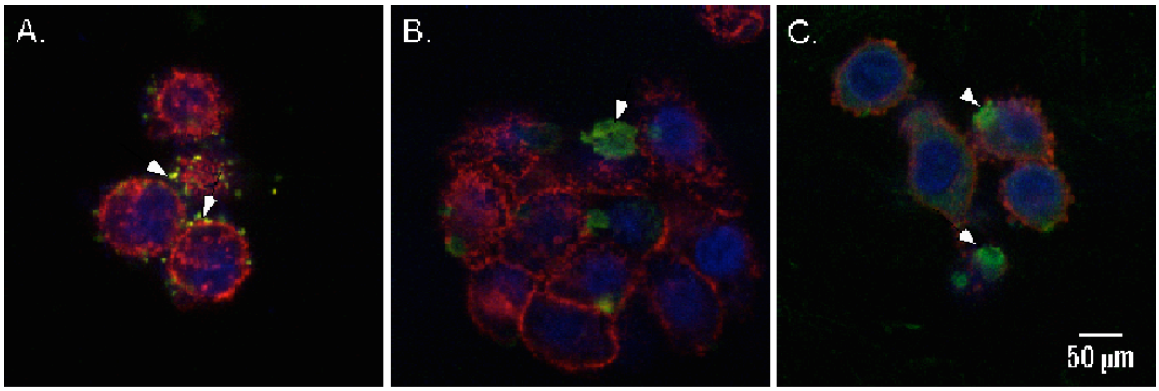

Figure 6: ROCK-II partially co-localizes with actin in NCM460 cells (A) but not in Caco-2 E (B) or SW620 cells (C). ROCK-II collections are formed at the tips of malignant cells (B, C). Actin is in red, ROCK-II is green, and DAPI staining for the nucleus is blue. Bar = 50 μm.

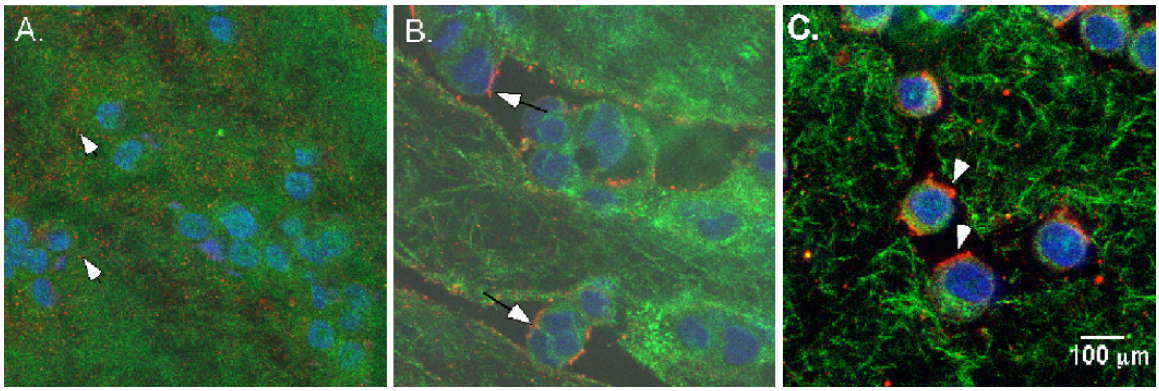

Figure 7: Collagen degradation was present in areas adjacent to heavy ROCK-II expression in malignant Caco-2 E cells (B) and SW620 cells (C). ROCK-II collections adjacent to voids within the matrix were not noted in non-malignant NCM460 cells (A). ROCK-II expression is red. Collagen autofluorescence is shown in green and DAPI staining for the nucleus is shown in blue. Bar = 100 µm.

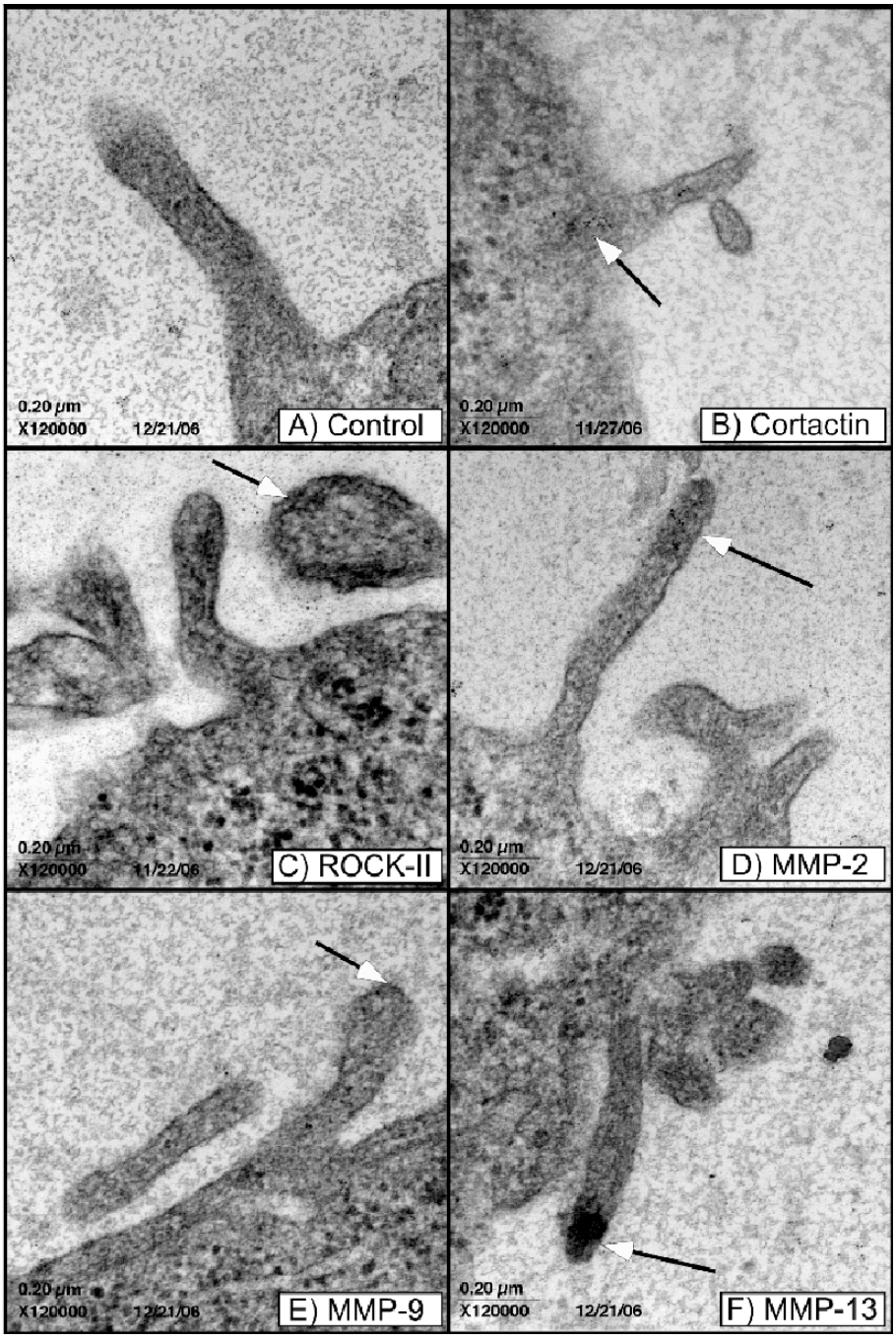

Figure 8: TEM images representing invadopodia structures in SW620 cells. Cells were stained for Cortactin (B), ROCK-II (C), MMP-2 (D), MMP-9 (E), and MMP-13 (F). Darker areas represent expression with arrows pointing to areas of expression. Coractin was present at the base of the structure; heavy ROCK-II expression was noted throughout the region; MMPs-2, 13 expression was noted at the tip of invadopodia. Some MMP-9 expression was observed, but expression was not as significant as MMP-2 or MMP-13. Bar = 0.2 µm.

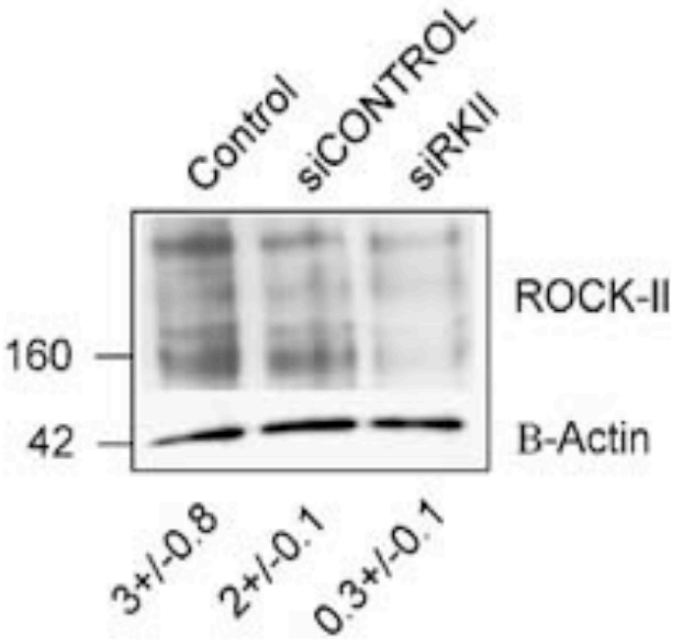

Figure 9: SW620 cells were transfected with ROCK-II siRNA to silence ROCK-II. A western blot confirming successful knockdown of ROCK-II. Densitometry was studied to quantify the relative expression for the untransfected (Control), mock transfection (siControl), and ROCK-II knockdown (siRKII). ROCK-II knockdown resulted in a significantly lower expression of ROCK-II compared to the other two conditions.

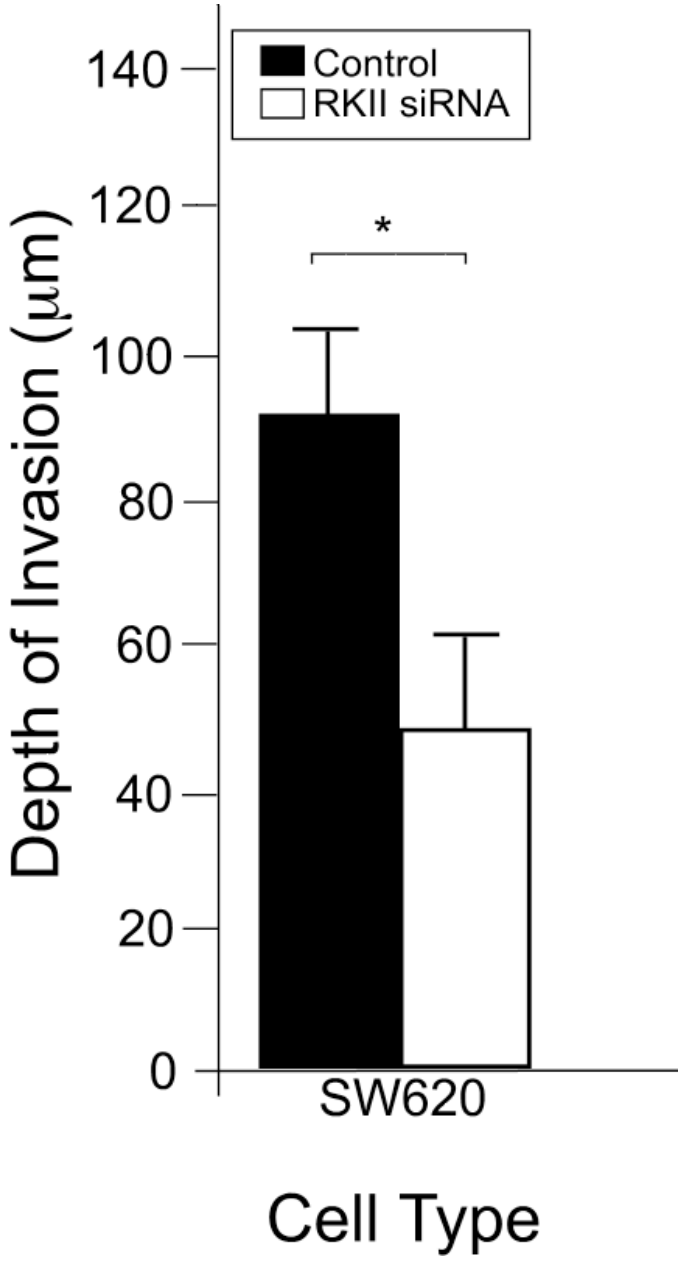

Figure 10: SW620 cells were transfected with ROCK-II siRNA and were allowed in migrate into collagen I scaffolds. ROCK-II knockdown resulted in a 50% decrease in SW620 invasion depth.

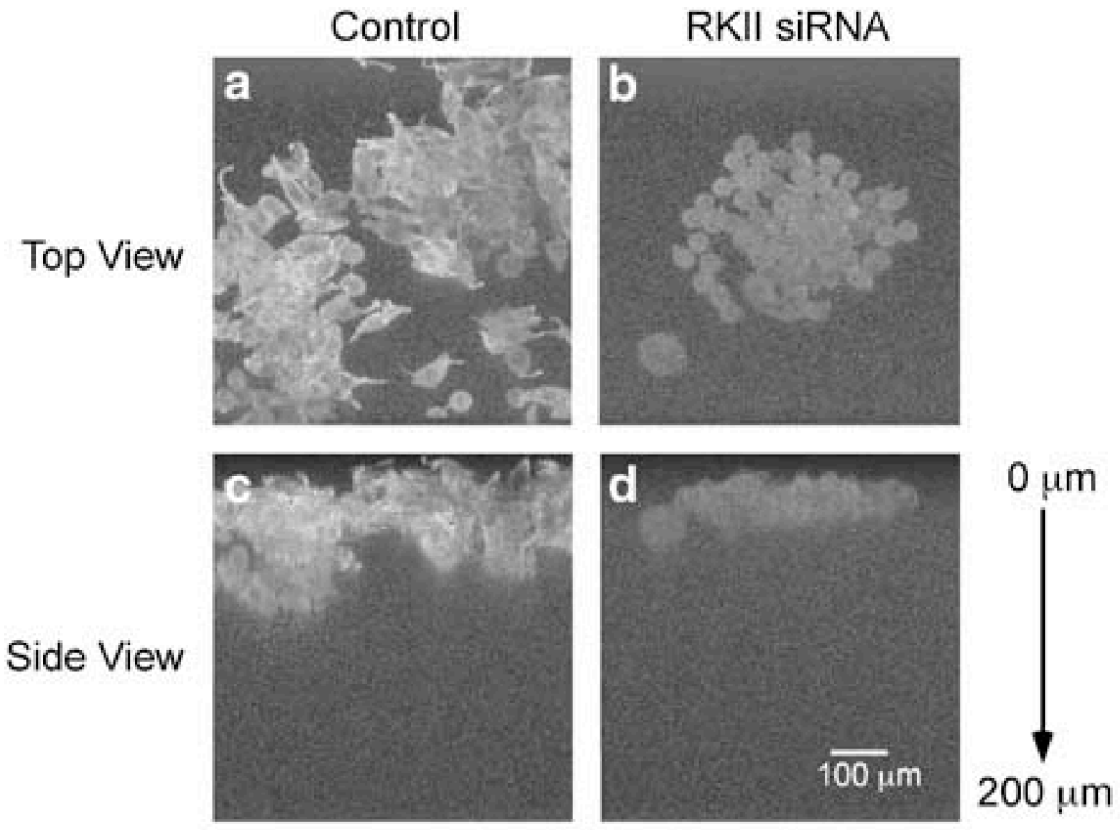

Figure 11: SW620 cells in collagen I scaffolds stained for F-actin. Untranfected cells (A, C) pentetrate deeper into the gel, have a more elongated morphology, and have greater actin signal than those transfected with ROCK-II siRNA (B, D). Bar = 100 μm.

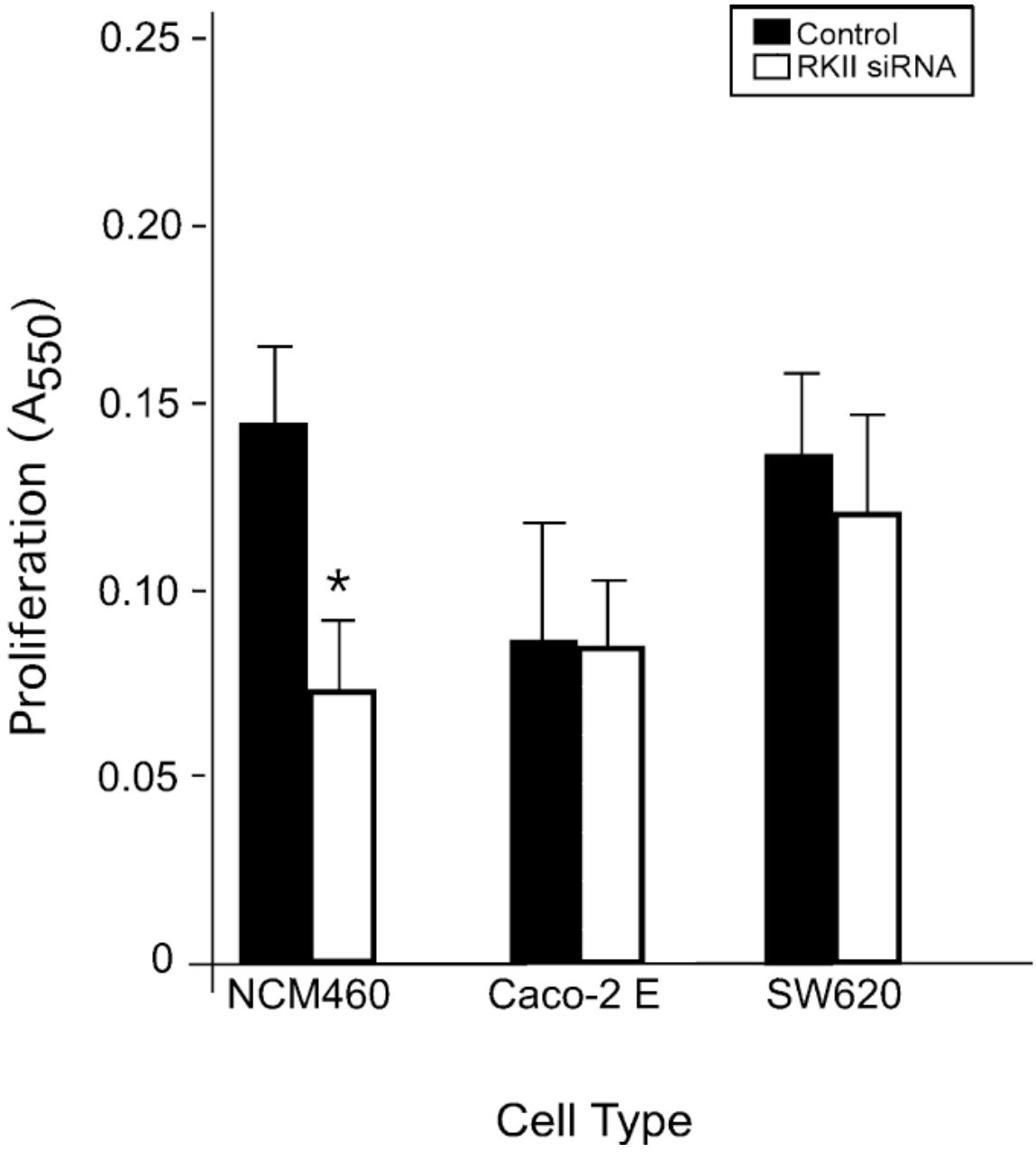

Figure 12: NCM460, Caco-2 E, and SW620 cells were seeded onto collagen I scaffolds. ROCK-II knockdown via siRNA reduced cell proliferation by 50% in non-malignant NCM460 cells. However, there was no significant impact due to ROCK-II knockdown in either malignant cell line.

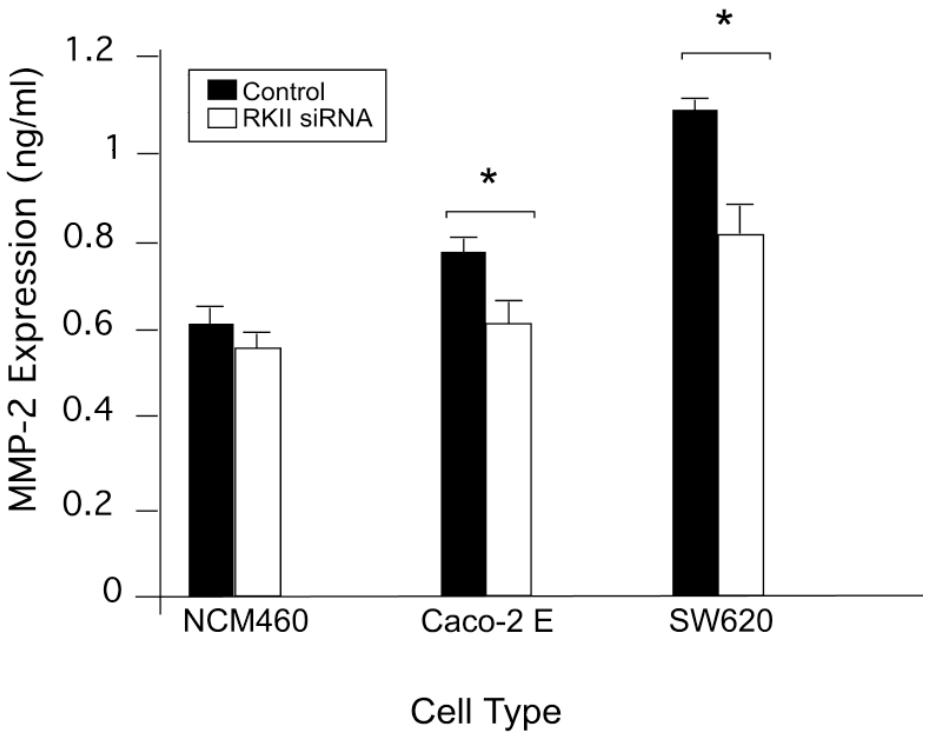

Figure 13: MMP-2 expression was quantified in NCM460, Caco-2 E, and SW620 cell lines. ROCK-II knockdown via siRNA did not have a significant impact on MMP-2 expression in non-malignant NCM460 cells. However, ROCK-II knockdown did significantly reduce MMP-2 expression in both Caco-2 E and SW620 cell lines.

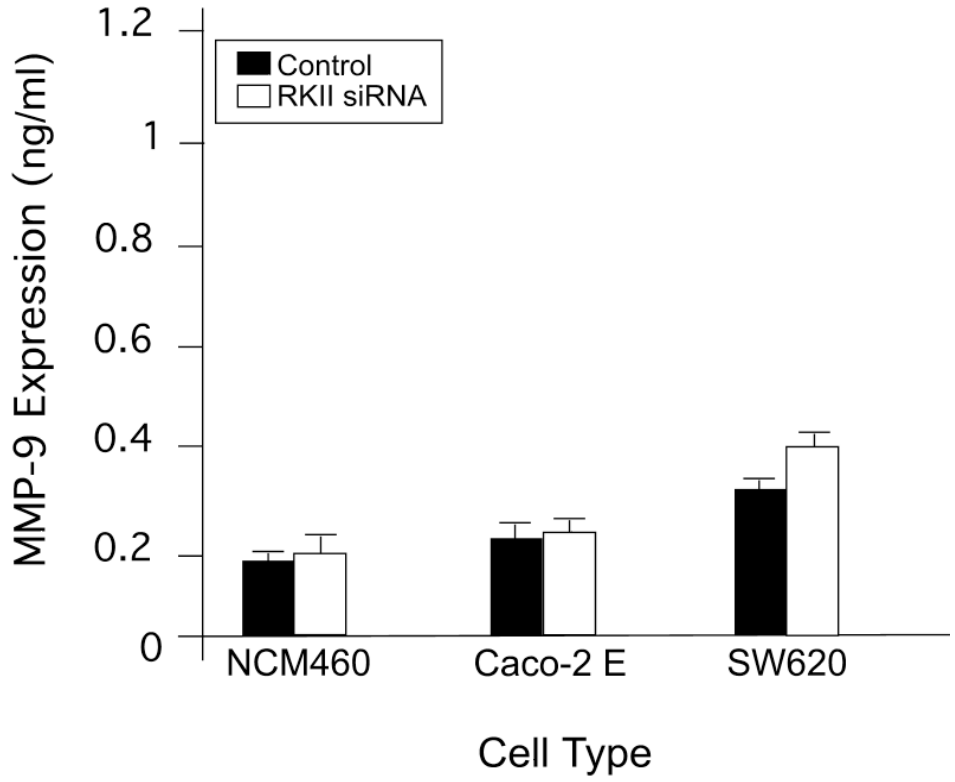

Figure 14: MMP-9 expression was quantified in NCM460, Caco-2 E, and SW620 cell lines. ROCK-II knockdown via siRNA did not have a significant impact on MMP-9 expression on any of the cell lines.

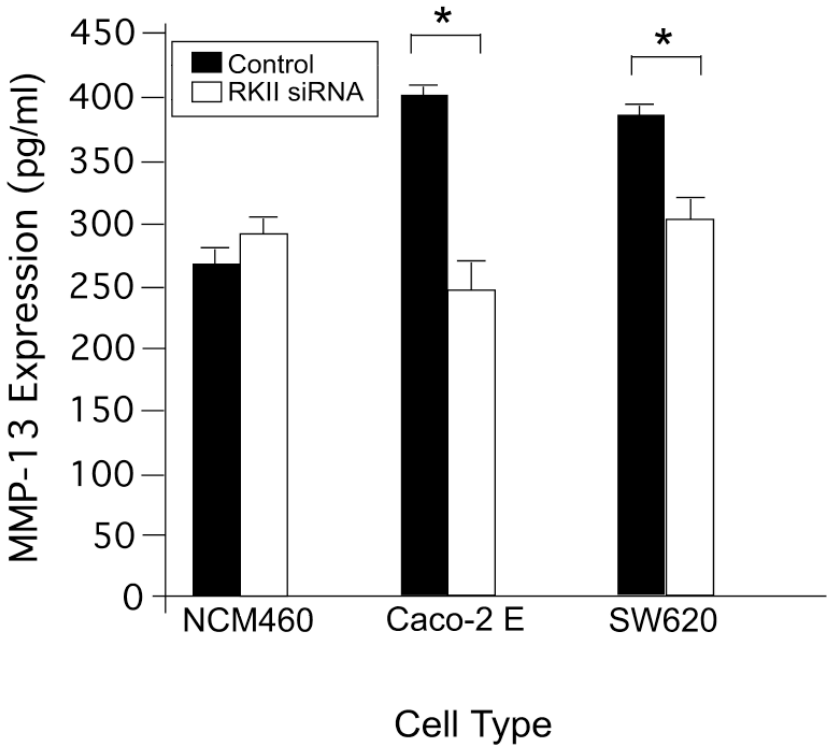

Figure 15: MMP-13 expression was quantified in NCM460, Caco-2 E, and SW620 cell lines. ROCK-II knockdown via siRNA did not have a significant impact on MMP-13 expression in non-malignant NCM460 cells. However, ROCK-II knockdown did significantly reduce MMP-13 expression in both Caco-2 E and SW620 cell lines.

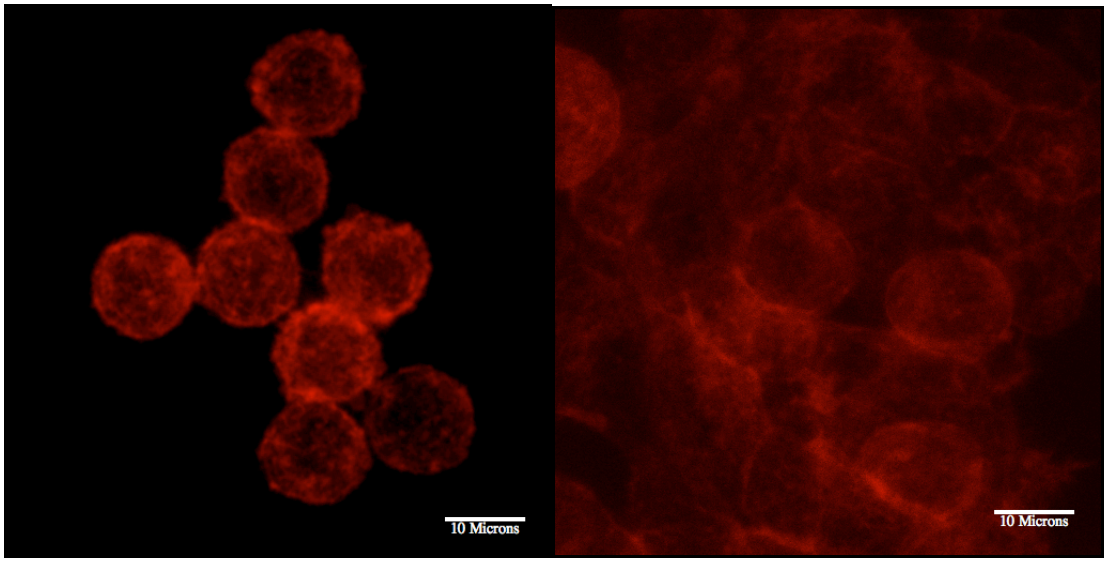

Figure 16: SW620 cells were seeded at different densities: 50,000 (left), and 250,000 cells/cm^2 (right). The lower seeding density (left) shows rounder cells with few cell-cell contacts. The greater seeding density allows for more cell-cell contact, creating a more epithelial state. Mag 600x.

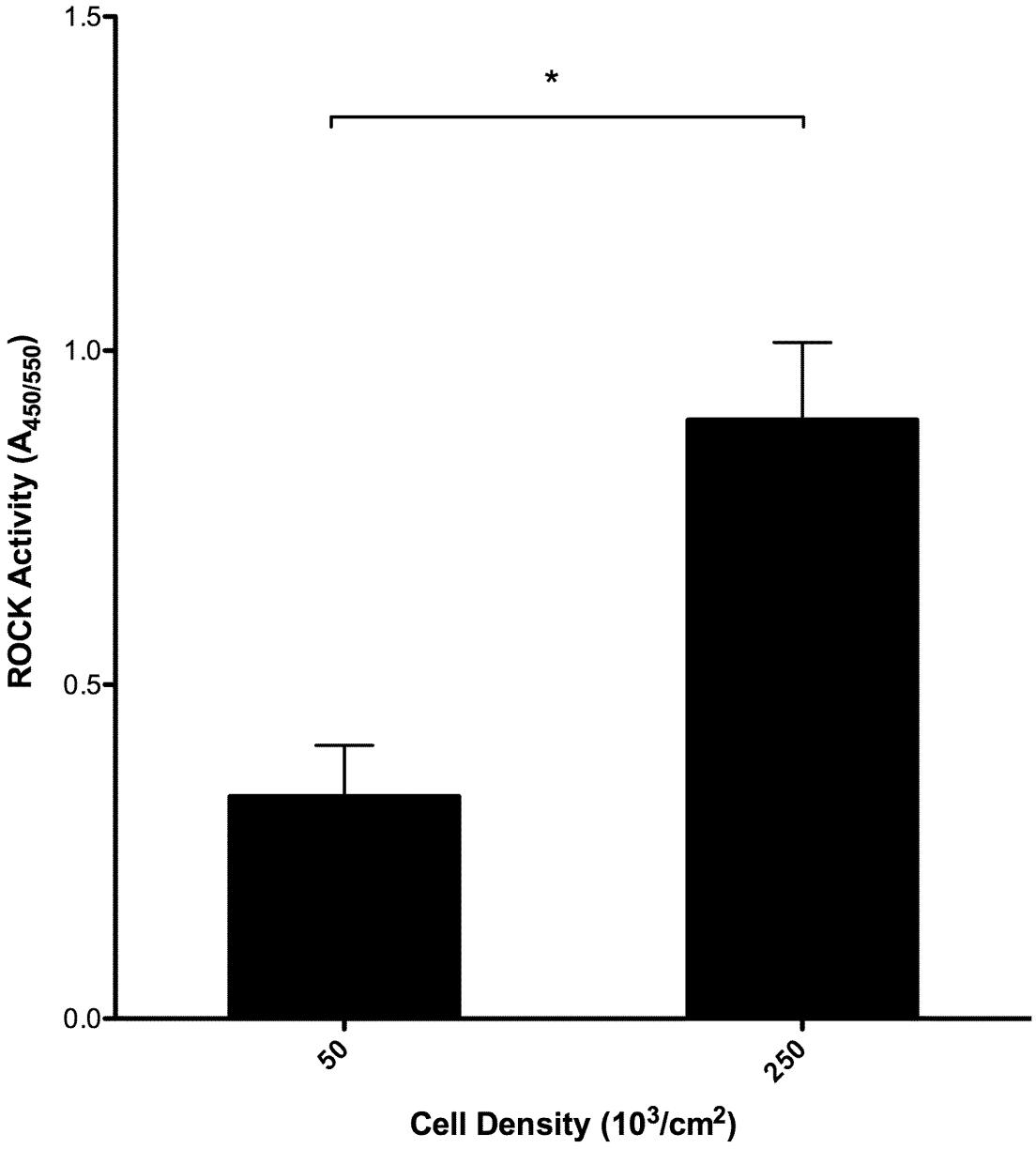

Figure 17: ROCK activities of SW620 cells seeded at 50,000 and 250,000 cells/cm2 and allowed to invade into 1.5 mg/ml collagen scaffolds. Cells seeded at the higher density had over double the ROCK activity compared to those seeded at the lower density. The number of cells were kept constant between the two conditions while the seeding area was altered.

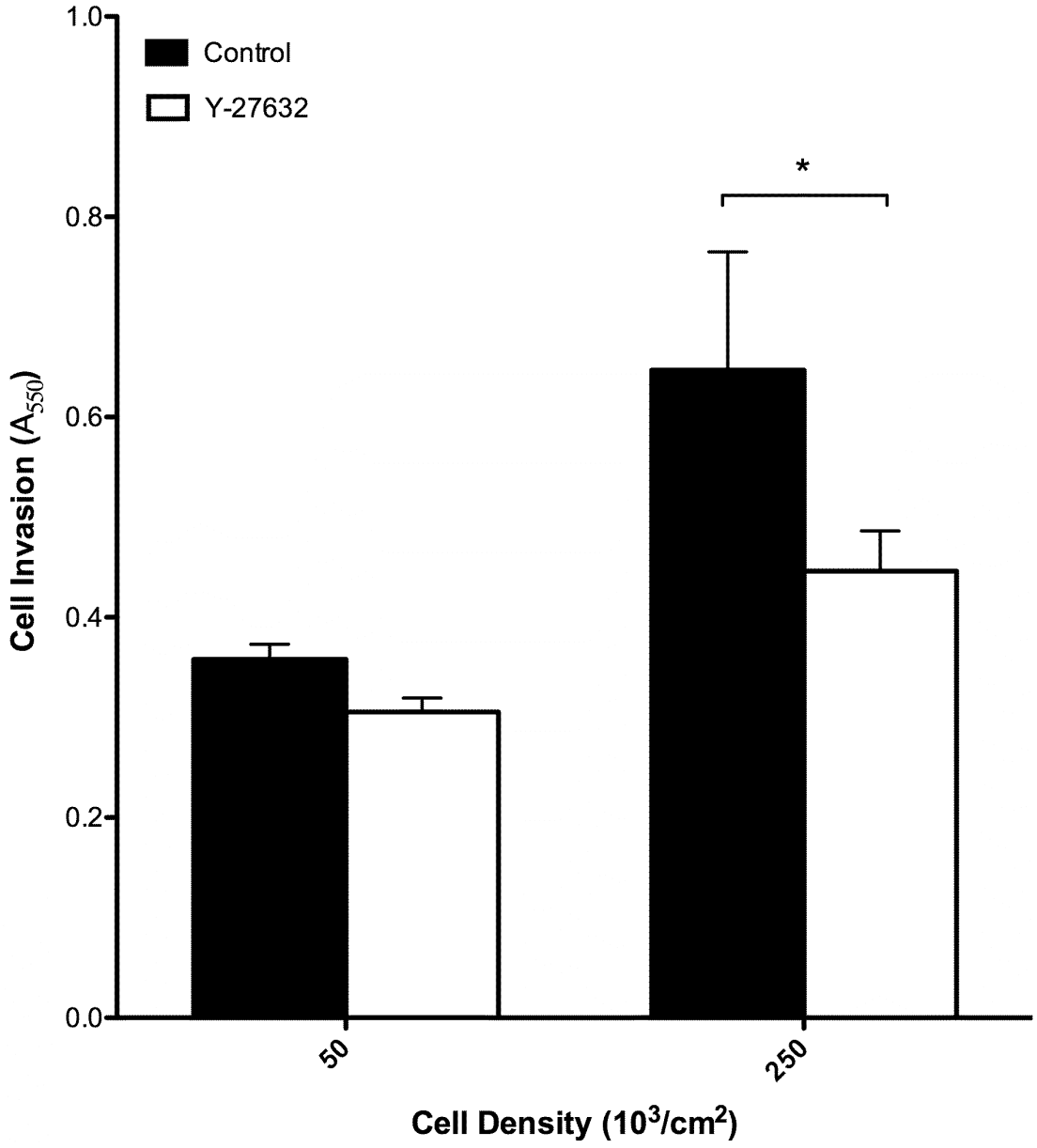

Figure 18: SW620 cells were seeded at densities of 50,000 and 250,000 cells/cm^2 onto Boyden chambers with an 8 µm pore membrane. The wells were treated with Y27632 to study the impact of ROCK inhibition on cell invasion in a low and high density environment. Treatment with Y27632 resulted in a 3.5-fold increase in cell invasion for cells seeded at 50,000 cells/cm^2.

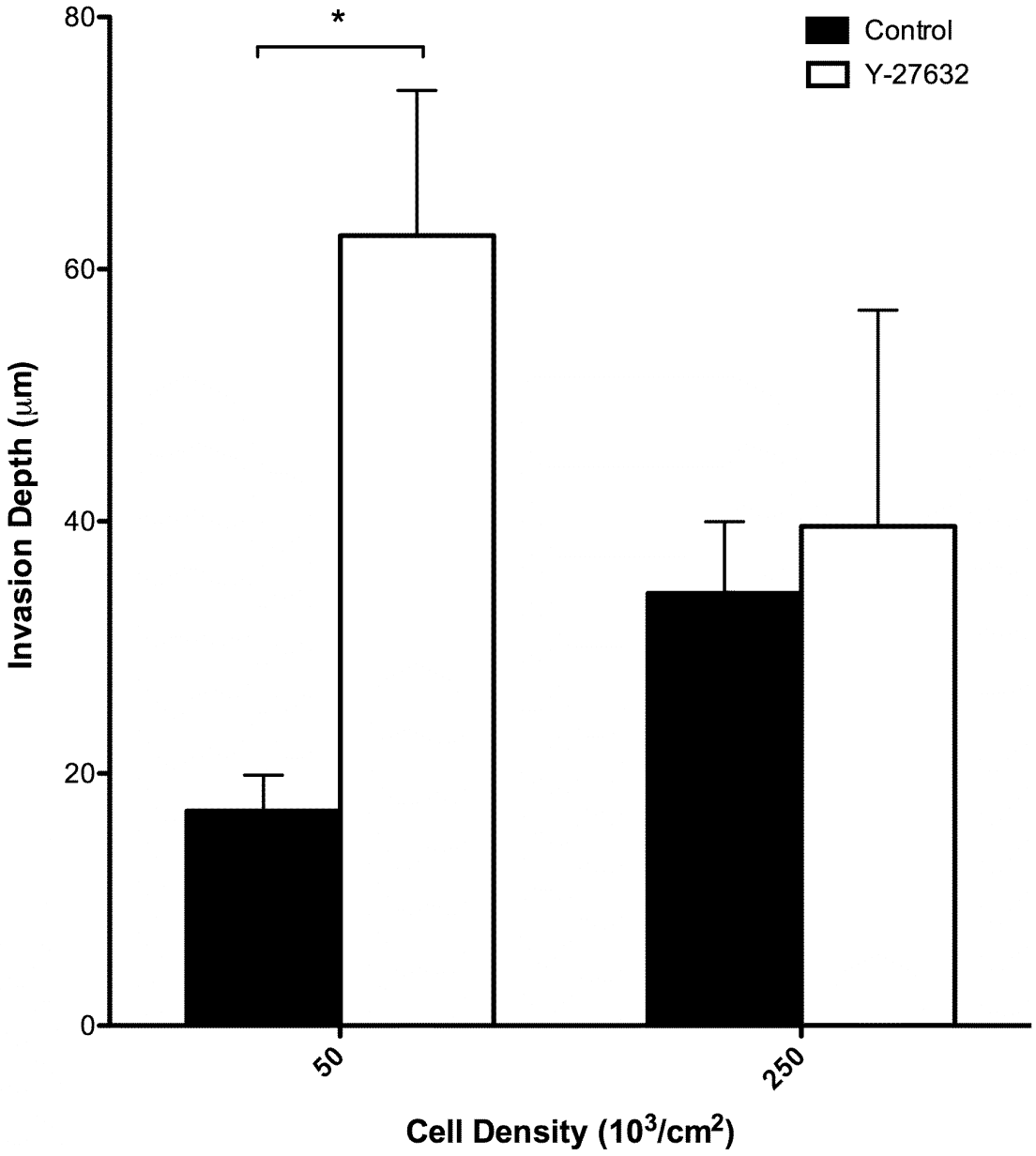

Figure 19: SW620 cells were seeded at densities of 50,000 and 250,000 cells/cm^2 onto 1.5 mg/ml collagen I gels. Scaffolds were treated with Y27632 to study the impact of ROCK-1 inhibition on cell invasion in a low and high density environment. Treatment with Y27632 resulted in a 3.5-fold increase in cell invasion for cells seeded at 50,000 cells/cm^2.

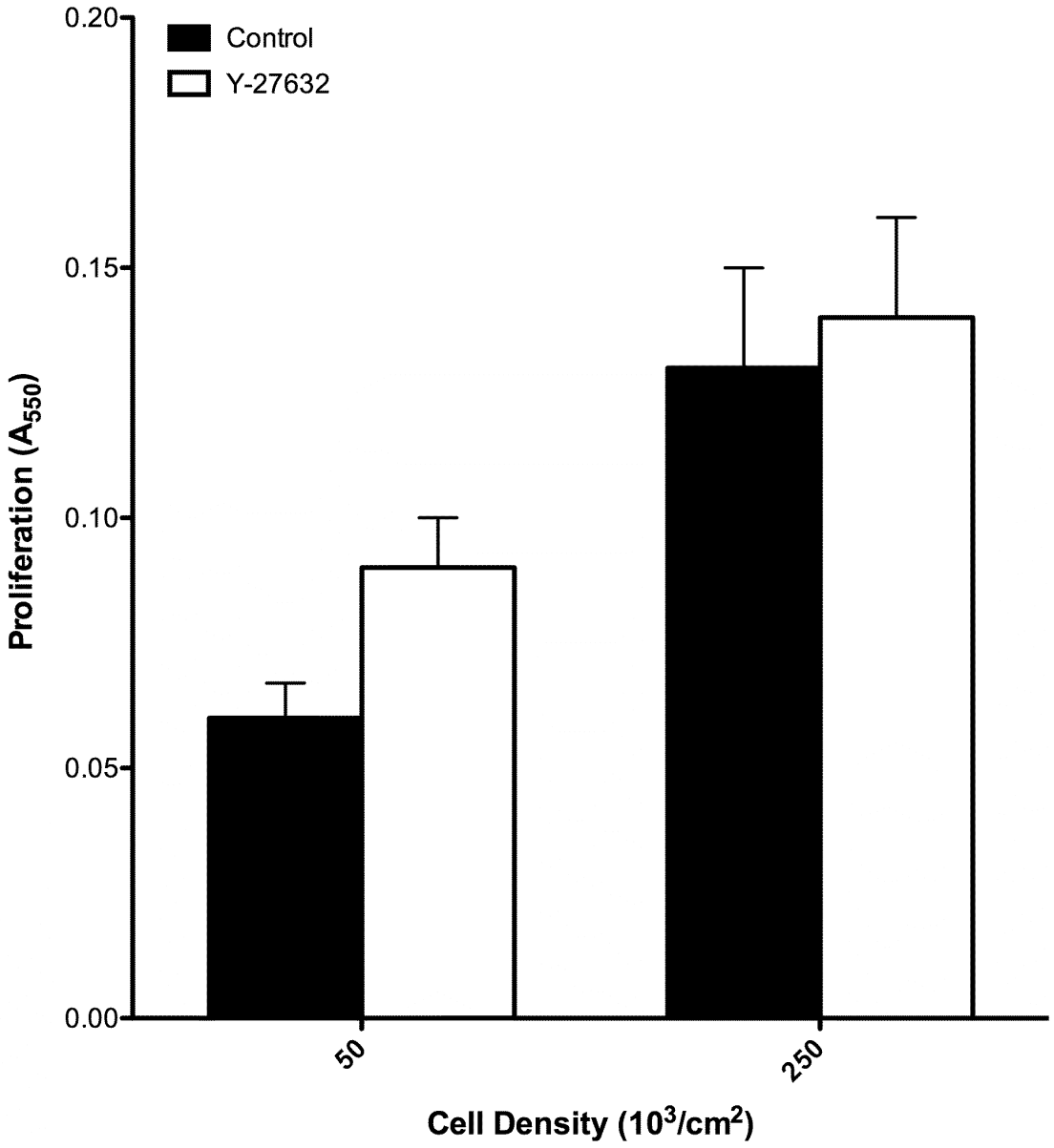

Figure 20: SW620 cells were seeded at densities of 50,000 and 250,000 cells/cm^2 onto 1.5 mg/ml collagen I gels. Scaffolds were treated with Y27632 to study the impact of ROCK-1 inhibition on cell proliferation in a low and high density environment. Treatment with Y27632 resulted in a modest increase in cell proliferation for cells seeded at 50,000 cells/cm^2 and no significant change for those seeded at 250,000 cells/cm^2. Furthermore, increasing cell density increased cell proliferation 2.5-fold for the untreated condition and 1.5-fold for those treated with Y-27632.

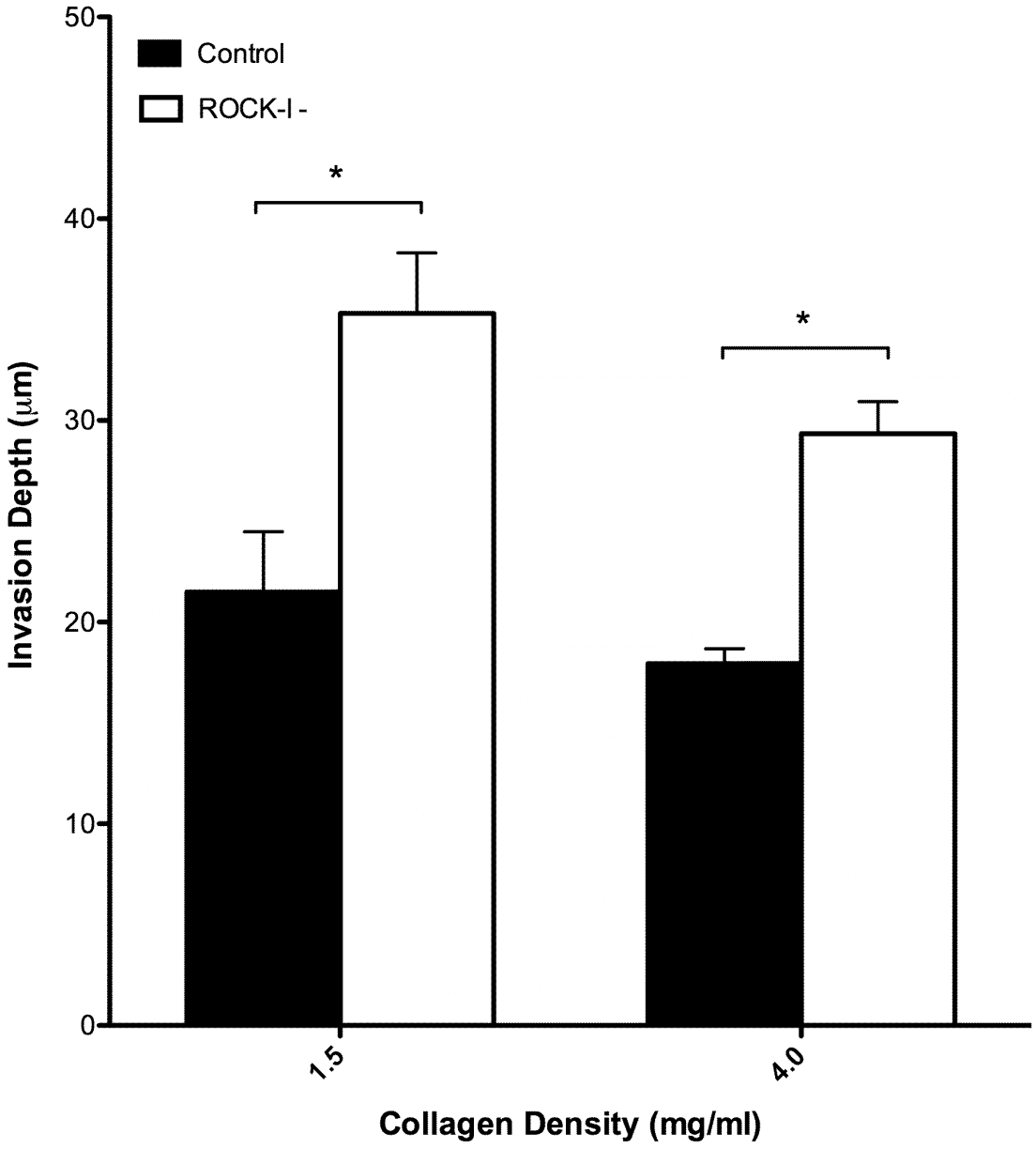

Figure 21: SW620 cells were seeded at densities 250,000 cells/cm^2 onto 1.5 and 4.0 mg/ml collagen I gels. ROCK-1 was knocked down via siRNA to study the impact of ROCK-I on cell invasion in a low and high density environment. ROCK-I knockdown resulted in a 60% increase in invasion for cells seeded in both 1.5 and 4.0 mg/ml scaffolds.

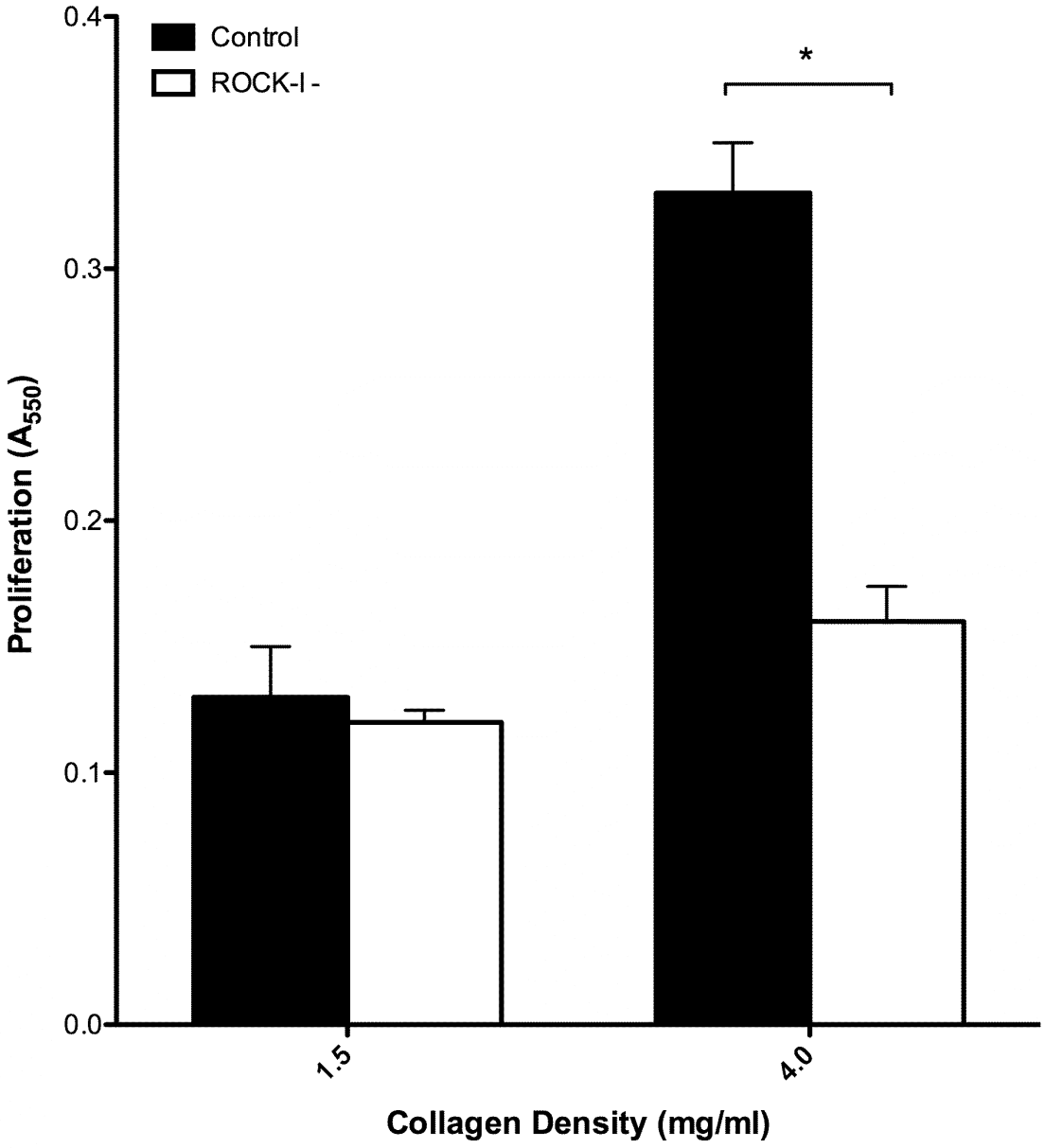

Figure 22: SW620 cells were seeded at densities 250,000 cells/cm^2 onto 1.5 and 4.0 mg/ml collagen I gels. ROCK-1 was knocked down via siRNA to study the impact of ROCK-I on cell invasion in a low and high density environment. Increasing collagen density resulted in a 2.5-fold increase in cell proliferation for the untransfected condition but only a 1.6-fold increase for those where ROCK-I expression was silenced. ROCK-I knockdown resulted in a 50% decrease in cell proliferation in cells in 4.0 mg/ml collagen I scaffolds.

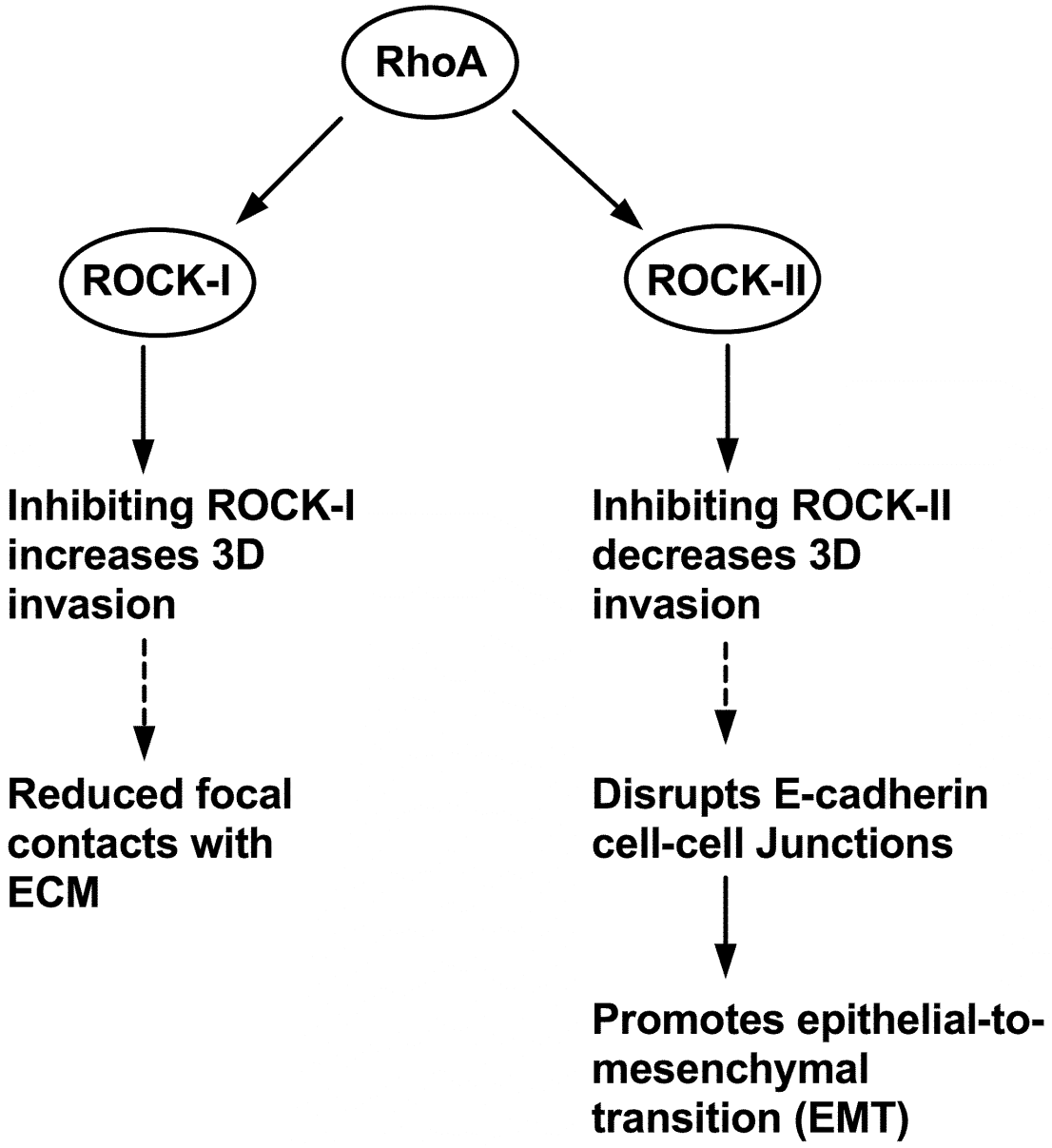

Figure 23: Diagram illustrating the findings of this dissertation. ROCK-I and ROCK-II contributed differently to colon cancer invasion within 3D scaffolds. This is due to the different function each protein on cell functions. ROCK-I is more greatly associated with focal adhesion and inhibiting this protein reduces the amount of focal adhesions. In 3D microenvironments, this results in an increase in invasion. ROCK-II has been shown to disrupt cell-cell junctions and therefore contributes to EMT. Inhibiting ROCK-II reduces this effect, which in turn reduces invasion.

CITED LITERATURE

Abbott, A. (2003). "Cell culture: biology's new dimension." Nature **424**(6951): 870-872.

Alberts, B. (2002). Molecular biology of the cell. New York, Garland Science.

Alvarez, B., P. J. Stroeken, et al. (2008). "Integrin Cytoplasmic domain-Associated Protein-1 (ICAP-1) promotes migration of myoblasts and affects focal adhesions." J Cell Physiol **214**(2): 474-482.

American Cancer Society (2010). Cancer Facts and Figures. American Cancer Society. Atlanta, GA.

American Joint Committee on Cancer (2002). AJCC Manual, Sixth Edition.

Artym, V. V., Y. Zhang, et al. (2006). "Dynamic interactions of cortactin and membrane type 1 matrix metalloproteinase at invadopodia: defining the stages of invadopodia formation and function." Cancer Res **66**(6): 3034-3043.

Astler, V. B. and F. A. Coller (1954). "The prognostic significance of direct extension of carcinoma of the colon and rectum." Ann Surg **139**(6): 846-852.

Bosman, F. T. (1995). "Prognostic value of pathological characteristics of colorectal cancer." Eur J Cancer **31A**(7-8): 1216-1221.

Bourguignon, L. Y., Z. Gunja-Smith, et al. (1998). "CD44v(3,8-10) is involved in cytoskeleton-mediated tumor cell migration and matrix metalloproteinase (MMP-9) association in metastatic breast cancer cells." J Cell Physiol **176**(1): 206-215.

Bowden, E. T., M. Barth, et al. (1999). "An invasion-related complex of cortactin, paxillin and PKCmu associates with invadopodia at sites of extracellular matrix degradation." Oncogene **18**(31): 4440-4449.

Bowden, E. T., E. Onikoyi, et al. (2006). "Co-localization of cortactin and phosphotyrosine identifies active invadopodia in human breast cancer cells." Exp Cell Res **312**(8): 1240-1253.

Boyd, N. F., L. J. Martin, et al. (2010). "Breast tissue composition and susceptibility to breast cancer." Journal of the National Cancer Institute **102**(16): 1224-1237.

Boyd, N. F., L. J. Martin, et al. (2009). "Mammographic density: a heritable risk factor for breast cancer." Methods Mol Biol **472**: 343-360.

Brower, V. (2010). "Breast density gains acceptance as breast cancer risk factor." Journal of the National Cancer Institute **102**(6): 374-375.

Bu, Q., H. M. Tang, et al. (2011). "[Expression of RhoC and ROCK-1 and their effects on MAPK and Akt proteins in prostate carcinoma]." Zhonghua zhong liu za zhi [Chinese journal of oncology] **33**(3): 202-206.

Buccione, R., J. D. Orth, et al. (2004). "Foot and mouth: podosomes, invadopodia and circular dorsal ruffles." Nat Rev Mol Cell Biol **5**(8): 647-657.

Camara, J. and G. Jarai (2010). "Epithelial-mesenchymal transition in primary human bronchial epithelial cells is Smad-dependent and enhanced by fibronectin and TNF-alpha." Fibrogenesis & tissue repair **3**(1): 2.

Chang, H. R., H. P. Huang, et al. (2010). "The suppressive effect of Rho kinase inhibitor, Y-27632, on oncogenic Ras/RhoA induced invasion/migration of human bladder cancer TSGH cells." Chemico-biological interactions **183**(1): 172-180.

Chao, A., M. J. Thun, et al. (2005). "Meat consumption and risk of colorectal cancer." JAMA **293**(2): 172-182.

Cheng, J. C. and P. C. Leung (2011). "Type I collagen down-regulates E-cadherin expression by increasing PI3KCA in cancer cells." Cancer letters **304**(2): 107-116.

Cho, E., S. A. Smith-Warner, et al. (2004). "Alcohol intake and colorectal cancer: a pooled analysis of 8 cohort studies." Ann Intern Med **140**(8): 603-613.

Chow, G., J. Tauler, et al. (2010). "Cytokines and growth factors stimulate hyaluronan production: role of hyaluronan in epithelial to mesenchymal-like transition in non-small cell lung cancer." Journal of biomedicine & biotechnology **2010**: 485468.

Chung, J. Y., J. A. Davis, et al. (2011). "Competitive enhancement of HGF-induced epithelial scattering by accessory growth factors." Experimental cell research **317**(3): 307-318.

Coleman, M. L., E. A. Sahai, et al. (2001). "Membrane blebbing during apoptosis results from caspase-mediated activation of ROCK I." Nat Cell Biol **3**(4): 339-345.

Coopman, P. J., M. T. Do, et al. (1998). "Phagocytosis of cross-linked gelatin matrix by human breast carcinoma cells correlates with their invasive capacity." Clin Cancer Res **4**(2): 507-515.

Croft, D. R., E. Sahai, et al. (2004). "Conditional ROCK activation in vivo induces tumor cell dissemination and angiogenesis." Cancer Res **64**(24): 8994-9001.

DeCosse, J. J., G. J. Tsioulias, et al. (1994). "Colorectal cancer: detection, treatment, and rehabilitation." CA Cancer J Clin **44**(1): 27-42.

Deng, L., G. Li, et al. (2010). "Rho-kinase inhibitor, fasudil, suppresses glioblastoma cell line progression in vitro and in vivo." Cancer biology & therapy **9**(11): 875-884.

Deryugina, E. I., B. Ratnikov, et al. (2001). "MT1-MMP initiates activation of pro-MMP-2 and integrin alphavbeta3 promotes maturation of MMP-2 in breast carcinoma cells." Exp Cell Res **263**(2): 209-223.

Doerner, A. M. and B. L. Zuraw (2009). "TGF-beta1 induced epithelial to mesenchymal transition (EMT) in human bronchial epithelial cells is enhanced by IL-1beta but not abrogated by corticosteroids." Respir Res **10**: 100.

Dukes, C. (1932). "The Classification of the Cancer of the Rectum." Journal of Pathological Bacteriology **35**(323).

Elnemr, A., Y. Yonemura, et al. (2003). "Expression of collagenase-3 (matrix metalloproteinase-13) in human gastric cancer." Gastric Cancer **6**(1): 30-38.

Flatmark, K., G. M. Maelandsmo, et al. (2004). "Twelve colorectal cancer cell lines exhibit highly variable growth and metastatic capacities in an orthotopic model in nude mice." Eur J Cancer **40**(10): 1593-1598.

Fukushima, M., M. Nakamuta, et al. (2005). "Fasudil hydrochloride hydrate, a Rho-kinase (ROCK) inhibitor, suppresses collagen production and enhances collagenase activity in hepatic stellate cells." Liver Int **25**(4): 829-838.

Hase, K., C. Shatney, et al. (1993). "Prognostic value of tumor "budding" in patients with colorectal cancer." Dis Colon Rectum **36**: 627-635.

Horiuchi, A., T. Imai, et al. (2003). "Up-regulation of small GTPases, RhoA and RhoC, is associated with tumor progression in ovarian carcinoma." Lab Invest **83**(6): 861-870.

Huang, S. and D. E. Ingber (2005). "Cell tension, matrix mechanics, and cancer development." Cancer cell **8**(3): 175-176.

Ishizaki, T., M. Uehata, et al. (2000). "Pharmacological properties of Y-27632, a specific inhibitor of rho-associated kinases." Mol Pharmacol **57**(5): 976-983.

Ivanov, A. I., S. N. Samarin, et al. (2009). "Protein kinase C activation disrupts epithelial apical junctions via ROCK-II dependent stimulation of actomyosin contractility." BMC Cell Biol **10**: 36.

Jemal, A., F. Bray, et al. (2011). "Global cancer statistics." CA: a cancer journal for clinicians **61**(2): 69-90.

Jeong, K. J., S. Y. Park, et al. (2012). "The Rho/ROCK pathway for lysophosphatidic acid-induced proteolytic enzyme expression and ovarian cancer cell invasion." Oncogene.

Jezierska, A. and T. Motyl (2009). "Matrix metalloproteinase-2 involvement in breast cancer progression: a mini-review." Med Sci Monit **15**(2): RA32-40.

Jordan, M. A. (2002). "Mechanism of action of antitumor drugs that interact with microtubules and tubulin." Curr Med Chem Anticancer Agents **2**(1): 1-17.

Kamai, T., T. Tsujii, et al. (2003). "Significant association of Rho/ROCK pathway with invasion and metastasis of bladder cancer." Clin Cancer Res **9**(7): 2632-2641.

Kamai, T., T. Yamanishi, et al. (2004). "Overexpression of RhoA, Rac1, and Cdc42 GTPases is associated with progression in testicular cancer." Clinical cancer research : an official journal of the American Association for Cancer Research **10**(14): 4799-4805.

Kang, M. H., J. S. Kim, et al. (2010). "BMP2 accelerates the motility and invasiveness of gastric cancer cells via activation of the phosphatidylinositol 3-kinase (PI3K)/Akt pathway." Experimental cell research **316**(1): 24-37.

Kenny, H. A. and E. Lengyel (2009). "MMP-2 functions as an early response protein in ovarian cancer metastasis." Cell Cycle **8**(5): 683-688.

Kerkela, E. and U. Saarialho-Kere (2003). "Matrix metalloproteinases in tumor progression: focus on basal and squamous cell skin cancer." Exp Dermatol **12**(2): 109-125.

Kidera, Y., M. Tsubaki, et al. (2010). "Reduction of lung metastasis, cell invasion, and adhesion in mouse melanoma by statin-induced blockade of the Rho/Rho-associated coiled-coil-containing protein kinase pathway." Journal of experimental & clinical cancer research : CR **29**: 127.

Kiss, C., J. Li, et al. (1997). "Assignment of the ARHA and GPX1 genes to human chromosome bands 3p21.3 by in situ hybridization and with somatic cell hybrids." Cytogenetics and cell genetics **79**(3-4): 228-230.

Klinge, U., R. Rosch, et al. (2006). "Different matrix micro-environments in colon cancer and diverticular disease." Int J Colorectal Dis.

Kuwano, H., T. Miyazaki, et al. (2004). "Cell density modulates the metastatic aggressiveness of a mouse colon cancer cell line, colon 26." Oncology **67**(5-6): 441-449.

Lane, J., T. A. Martin, et al. (2008). "The expression and prognostic value of ROCK I and ROCK II and their role in human breast cancer." Int J Oncol **33**(3): 585-593.

Leeman, M. F., J. A. McKay, et al. (2002). "Matrix metalloproteinase 13 activity is associated with poor prognosis in colorectal cancer." J Clin Pathol **55**(10): 758-762.

Leibovitz, A., J. C. Stinson, et al. (1976). "Classification of human colorectal adenocarcinoma cell lines." Cancer Res **36**(12): 4562-4569.

Leung, T., X. Q. Chen, et al. (1996). "The p160 RhoA-binding kinase ROK alpha is a member of a kinase family and is involved in the reorganization of the cytoskeleton." Molecular and cellular biology **16**(10): 5313-5327.

Li, B., W. D. Zhao, et al. (2006). "Involvement of Rho/ROCK signalling in small cell lung cancer migration through human brain microvascular endothelial cells." FEBS letters **580**(17): 4252-4260.

Liao, J. K., M. Seto, et al. (2007). "Rho kinase (ROCK) inhibitors." J Cardiovasc Pharmacol **50**(1): 17-24.

Libra, M., A. Scalisi, et al. (2009). "Uterine cervical carcinoma: role of matrix metalloproteinases (review)." Int J Oncol **34**(4): 897-903.

Lin, C. Y., P. H. Tsai, et al. "Matrix metalloproteinase-9 cooperates with transcription factor Snail to induce epithelial-mesenchymal transition." Cancer Sci **102**(4): 815-827.

Lin, C. Y., P. H. Tsai, et al. (2011). "Matrix metalloproteinase-9 cooperates with transcription factor Snail to induce epithelial-mesenchymal transition." Cancer science **102**(4): 815-827.

Linder, S. (2007). "The matrix corroded: podosomes and invadopodia in extracellular matrix degradation." Trends Cell Biol **17**(3): 107-117.

Liu, S., R. H. Goldstein, et al. (2009). "Inhibition of rho-associated kinase signaling prevents breast cancer metastasis to human bone." Cancer Res **69**(22): 8742-8751.

Lock, F. E. and N. A. Hotchin (2009). "Distinct roles for ROCK1 and ROCK2 in the regulation of keratinocyte differentiation." PLoS One **4**(12): e8190.

Marx, J. (2006). "Cell biology. Podosomes and invadopodia help mobile cells step lively." Science **312**(5782): 1868-1869.

McBeath, R., D. M. Pirone, et al. (2004). "Cell shape, cytoskeletal tension, and RhoA regulate stem cell lineage commitment." Dev Cell **6**(4): 483-495.

McConkey, D. J., W. Choi, et al. (2009). "Role of epithelial-to-mesenchymal transition (EMT) in drug sensitivity and metastasis in bladder cancer." Cancer Metastasis Rev **28**(3-4): 335-344.

Meriane, M., S. Duhamel, et al. (2006). "Cooperation of matrix metalloproteinases with the RhoA/Rho kinase and mitogen-activated protein kinase kinase-1/extracellular signal-regulated kinase signaling pathways is required for the sphingosine-1-phosphate-induced mobilization of marrow-derived stromal cells." Stem Cells **24**(11): 2557-2565.

Mizoue, T., K. Tanaka, et al. (2006). "Alcohol drinking and colorectal cancer risk: an evaluation based on a systematic review of epidemiologic evidence among the Japanese population." Jpn J Clin Oncol **36**(9): 582-597.

Moyer, M. P., J. Stauffer, et al. (1996). "NCM460, a normal human colon mucosal epithelial cell line." In Vitro Cell Devel Biol (Animal) **32**: 315-317.

Mueller, B. K., H. Mack, et al. (2005). "Rho kinase, a promising drug target for neurological disorders." Nat Rev Drug Discov **4**(5): 387-398.

Nagase, H. (1998). "Cell surface activation of progelatinase A (proMMP-2) and cell migration." Cell Res **8**(3): 179-186.

Nagi, C. and I. J. Bleiweiss (2007). "Invadopodia and cancer cell migration." Adv Anat Pathol **14**(1): 55-56.

Nakabayashi, H. and K. Shimizu (2011). "HA1077, a Rho kinase inhibitor, suppresses glioma-induced angiogenesis by targeting the Rho-ROCK and the mitogen-activated protein kinase kinase/extracellular signal-regulated kinase (MEK/ERK) signal pathways." Cancer science **102**(2): 393-399.

Nakagawa, H., K. Yoshioka, et al. (2005). "Intrathecal administration of Y-27632, a specific rho-associated kinase inhibitor, for rat neoplastic meningitis." Molecular cancer research : MCR **3**(8): 425-433.

Nakagawa, O., K. Fujisawa, et al. (1996). "ROCK-I and ROCK-II, two isoforms of Rho-associated coiled-coil forming protein serine/threonine kinase in mice." FEBS Lett **392**(2): 189-193.

Nannuru, K. C., M. Futakuchi, et al. (2010). "Matrix metalloproteinase (MMP)-13 regulates mammary tumor-induced osteolysis by activating MMP9 and transforming growth factor-beta signaling at the tumor-bone interface." Cancer research **70**(9): 3494-3504.

Nelson, C. M. and C. S. Chen (2002). "Cell-cell signaling by direct contact increases cell proliferation via a PI3K-dependent signal." FEBS letters **514**(2-3): 238-242.

Ogata, S., K. Morishige, et al. (2009). "Fasudil inhibits lysophosphatidic acid-induced invasiveness of human ovarian cancer cells." Int J Gynecol Cancer **19**(9): 1473-1480.

Olson, M. F. (2008). "Applications for ROCK kinase inhibition." Curr Opin Cell Biol **20**(2): 242-248.

Pardee, A. B. (1989). "G1 events and regulation of cell proliferation." Science **246**(4930): 603-608.

Paszek, M. J., N. Zahir, et al. (2005). "Tensional homeostasis and the malignant phenotype." Cancer Cell **8**(3): 241-254.

Przybylo, J. A. and D. C. Radisky (2007). "Matrix metalloproteinase-induced epithelial-mesenchymal transition: tumor progression at Snail's pace." Int J Biochem Cell Biol **39**(6): 1082-1088.

Pyke, C., S. Salo, et al. (1995). "Laminin-5 is a marker of invading cancer cells in some human carcinomas and is coexpressed with the receptor for urokinase plasminogen activator in budding cancer cells in colon adenocarcinomas." Cancer Res **55**(18): 4132-4139.

Radisky, E. S. and D. C. Radisky (2010). "Matrix metalloproteinase-induced epithelial-mesenchymal transition in breast cancer." Journal of mammary gland biology and neoplasia **15**(2): 201-212.

Ramachandran, C., R. V. Patil, et al. (2011). "Rho-Rho kinase pathway in the actomyosin contraction and cell-matrix adhesion in immortalized human trabecular meshwork cells." Molecular vision **17**: 1877-1890.

Riento, K. and A. J. Ridley (2003). "Rocks: multifunctional kinases in cell behaviour." Nat Rev Mol Cell Biol **4**(6): 446-456.

Sahai, E., R. Garcia-Medina, et al. (2007). "Smurf1 regulates tumor cell plasticity and motility through degradation of RhoA leading to localized inhibition of contractility." J Cell Biol **176**(1): 35-42.

Sahai, E. and C. J. Marshall (2002). "ROCK and Dia have opposing effects on adherens junctions downstream of Rho." Nat Cell Biol **4**(6): 408-415.

Sahai, E. and C. J. Marshall (2003). "Differing modes of tumour cell invasion have distinct requirements for Rho/ROCK signalling and extracellular proteolysis." Nat Cell Biol **5**(8): 711-719.

Sahai, E., M. F. Olson, et al. (2001). "Cross-talk between Ras and Rho signalling pathways in transformation favours proliferation and increased motility." The EMBO journal **20**(4): 755-766.

Samarin, S. N., A. I. Ivanov, et al. (2007). "Rho/Rho-associated kinase-II signaling mediates disassembly of epithelial apical junctions." Mol Biol Cell **18**(9): 3429-3439.

Schrader, J., T. T. Gordon-Walker, et al. (2011). "Matrix stiffness modulates proliferation, chemotherapeutic response, and dormancy in hepatocellular carcinoma cells." Hepatology **53**(4): 1192-1205.

Sebbagh, M., C. Renvoize, et al. (2001). "Caspase-3-mediated cleavage of ROCK I induces MLC phosphorylation and apoptotic membrane blebbing." Nat Cell Biol **3**(4): 346-352.

Siegel, R., E. Ward, et al. (2011). "Cancer statistics, 2011: the impact of eliminating socioeconomic and racial disparities on premature cancer deaths." CA: a cancer journal for clinicians **61**(4): 212-236.

Strate, L. L. and S. Syngal (2005). "Hereditary colorectal cancer syndromes." Cancer Causes Control **16**(3): 201-213.

Sun, S., J. Wise, et al. (2004). "Human fibroblast migration in three-dimensional collagen gel in response to noninvasive electrical stimulus. I. Characterization of induced three-dimensional cell movement." Tissue Eng **10**(9-10): 1548-1557.

Suzuki, Y., M. Shibuya, et al. (2007). "A postmarketing surveillance study of fasudil treatment after aneurysmal subarachnoid hemorrhage." Surg Neurol **68**(2): 126-131; discussion 131-122.

Szarvas, T., M. Becker, et al. (2011). "Elevated serum matrix metalloproteinase 7 levels predict poor prognosis after radical prostatectomy." International journal of cancer. Journal international du cancer **128**(6): 1486-1492.

Tamura, M., H. Nakao, et al. (2005). "Development of specific Rho-kinase inhibitors and their clinical application." Biochim Biophys Acta **1754**(1-2): 245-252.

Tan, T. K., G. Zheng, et al. (2010). "Macrophage matrix metalloproteinase-9 mediates epithelial-mesenchymal transition in vitro in murine renal tubular cells." The American journal of pathology **176**(3): 1256-1270.

Tawara, S. and H. Shimokawa (2007). "Progress of the study of rho-kinase and future perspective of the inhibitor." Yakugaku Zasshi **127**(3): 501-514.

Torka, R., F. Thuma, et al. (2006). "ROCK signaling mediates the adoption of different modes of migration and invasion in human mammary epithelial tumor cells." Exp Cell Res **312**(19): 3857-3871.

Turner, N. A., D. J. O'Regan, et al. (2005). "Simvastatin inhibits MMP-9 secretion from human saphenous vein smooth muscle cells by inhibiting the RhoA/ROCK pathway and reducing MMP-9 mRNA levels." Faseb J **19**(7): 804-806.

Vishnubhotla, R., S. Sun, et al. (2007). "ROCK-II mediates colon cancer invasion via regulation of MMP-2 and MMP-13 at the site of invadopodia as revealed by multiphoton imaging." Lab Invest **87**(11): 1149-1158.

Wang, L., L. Xue, et al. "Effects of ROCK inhibitor, Y-27632, on adhesion and mobility in esophageal squamous cell cancer cells." Mol Biol Rep **37**(4): 1971-1977.

Weaver, A. M. (2006). "Invadopodia: specialized cell structures for cancer invasion." Clin Exp Metastasis **23**(2): 97-105.

Weaver, A. M. (2006). "Invadopodia: Specialized Cell Structures for Cancer Invasion." Clinical and Experimental Metastasis **In Press**.

Wells, R. G. (2008). "The role of matrix stiffness in regulating cell behavior." Hepatology **47**(4): 1394-1400.

Wood, C. B., C. R. Gillis, et al. (1981). "Local tumor invasion as a prognostic factor in colorectal cancer." Br J Surg **68**: 326-328.

Wozniak, M. A., R. Desai, et al. (2003). "ROCK-generated contractility regulates breast epithelial cell differentiation in response to the physical properties of a three-dimensional collagen matrix." The Journal of cell biology. **163**(3): 583-595.

Wyckoff, J. B., S. E. Pinner, et al. (2006). "ROCK- and myosin-dependent matrix deformation enables protease-independent tumor-cell invasion in vivo." Curr Biol **16**(15): 1515-1523.

Yamaguchi, H., F. Pixley, et al. (2006). "Invadopodia and podosomes in tumor invasion." Eur J Cell Biol **85**(3-4): 213-218.

Yang, X., Y. Liu, et al. "The Rho kinase inhibitor fasudil inhibits the migratory behaviour of 95-D lung carcinoma cells." Biomed Pharmacother **64**(1): 58-62.

Yang, X., Y. Liu, et al. (2010). "The Rho kinase inhibitor fasudil inhibits the migratory behaviour of 95-D lung carcinoma cells." Biomedicine & pharmacotherapy = Biomedecine & pharmacotherapie **64**(1): 58-62.

Yao, H. W., Q. M. Xie, et al. (2004). "TGF-beta1 induces alveolar epithelial to mesenchymal transition in vitro." Life Sci **76**(1): 29-37.

Yen, P. L., D. R. Chen, et al. (2011). "Development of a stiffness measurement accessory for ultrasound in breast cancer diagnosis." Medical engineering & physics **33**(9): 1108-1119.

Ying, H., S. L. Biroc, et al. (2006). "The Rho kinase inhibitor fasudil inhibits tumor progression in human and rat tumor models." Mol Cancer Ther **5**(9): 2158-2164.

Yoneda, A., H. A. Multhaupt, et al. (2005). "The Rho kinases I and II regulate different aspects of myosin II activity." J Cell Biol **170**(3): 443-453.

Zhang, M., Z. Zhang, et al. (2009). "TGF-beta1 induces human bronchial epithelial cell-to-mesenchymal transition in vitro." Lung **187**(3): 187-194.

Zhao, Z. and S. A. Rivkees (2004). "Rho-associated kinases play a role in endocardial cell differentiation and migration." Dev Biol **275**(1): 183-191.

VITA

NAME: Ramana Venkata Vishnubhotla

EDUCATION: B.S., Chemical Engineering, University of Michigan, Ann Arbor, Michigan, 2002

Ph.D., Bioengineering, University of Illinois at Chicago, Chicago, Illinois, 2012

PUBLICATIONS: Vishnubhotla, R. and Sun, S. Huq, J. Bulic, M. Ramesh, A. Guzman, G. Cho, M. Glover, S.C. ROCK-II Mediates Colon Cancer Invasion Via Regulation of MMP-2 and 13 at the Site of Invadopodia As Revealed By Multiphoton Imaging. Lab Invest. 7(11):1149-58.

Ramana Vishnubhotla, Shruthi Bharadwaj, Shan Sun, Vitali Metlushko, Sarah C. Glover. Treatment with Y-27632, a ROCK Inhibitor, Increases the Pro-Invasive Nature of SW620 Cells on 3-D Collagen Type-1 Matrix. International Journal of Cell Biology, 2012. (In Review)

Rapier, R. Huq, J. Vishnubhotla, R. Bulic, M. Perrault, CM. Metlushko, V. Cho, M. Tran Son Tay, R. Glover, SC. The Extracellular Matrix Microtopography Drives Critical Changes in Cellular Motility and Rho A Activity in Colon Cancer Cells. Cancer Cell International. 10:24.

Shruthi Bharadwaj, Ramana Vishnubhotla, Sun Shan, Chinmay Chauhan, Michael Cho, and Sarah C. Glover, “Higher Molecular Weight Polyethylene Glycol Increases Cell Proliferation While Improving Barrier Function in an In Vitro Colon Cancer Model,” Journal of Biomedicine and Biotechnology, vol. 2011.

S. Bharadwaj, V. Nekrasov, R. Vishnubhotla, C. Foster and S. Glover, "Commensal E. Coli Strains Uniquely Alter the ECM Topography Independent of Colonic Epithelial Cells," Journal of Biomaterials and Nanobiotechnology, Vol. 3 No. 1, pp. 70-78.

ABSTRACTS:

Glover, SC. Huq, J. Vishnubhotla, R. Bulic, M. Sun, S. Cho, M. Guzman,, G. ROCK II Modulates Tumor Cell Invasion in Colon Cancer via Invadopodia [Abstract]. AGA Stem Cell Meeting, 2006, Tyson's Corner, VA.

Glover SC, Huq J, Vishnubhotla R, Cho MR, Sun S. ROCK II mediates colon cancer cell invasion in 3D [Abstract]. The 2006 Annual Fall Meeting of the Biomedical Engineering Society. Chicago, IL.

Glover, SC. Huq, J. Vishnubhotla, R. Bulic, M. Sun, S. Cho, M. Guzman,, G. ROCK II Modulates Tumor Cell Invasion in Colon Cancer via Invadopodia [Abstract]. 46th Annual Meeting of the American Society for Cell Biology in San Diego, CA.

Bulic, M. Vishnubhotla, R. Roxas, J. L. Huq, J. Sun, S.; Cho, M. Viswanathan, V. K. Glover, S. C. Transient EPEC Infection of Colon Cancer Cells in 3D Scaffolds Increases Cell Invasion via the Influence of the T3SS on ROCK Signaling. Gastroenterology 2007: 132(4) A304.

Vishnubhotla, Ramana; Bulic, Marinka; Huq, Jameela; Sun, Shan; Cho, Michael; Glover, S. C. ROCK II Mediates Colon Cancer Invasion in a 3D In Vitro Model. Gastroenterology 2007: 132(4) A303.

Huq, J. Mecum, R. Bulic, M. Perrault, C. Vishnubhotla, R. Sun, S. Cho, M. Tran Son Tay, R. Glover, SC Surface Microtopographies Identified in Colon Cancer Critically Modulate Tumor Cell Behavior Via Rho. The 2007 Annual Fall Meeting of the Biomedical Engineering Society. Los Angeles, CA.

Bulic, M. Vishnubhotla, R. Huq, J. Sun, S. Roxas, J. L. Cho, M. Viswanathan, V.K. Glover, SC. Transient Infection with a Common Enteric Pathogen Increases Colon Cancer Invasion via ROCK Signaling in an In Vitro Model [Abstract]. 47th Annual Meeting of the American Society for Cell Biology in Washington, DC.

Sarah C. Glover, Marinka Bulic, Ramana V. Vishnubhotla, V. K. Viswanathan1, Michael Cho, Jennifer L. Roxas, Rebecca Mecum, Igor Titushkin A Loss of Symbiosis with Certain

Strains of Commensal E. coli Leads to Increased Colon Cancer Invasion in an In Vitro Colon Cancer Model via activation of Rac and MMP-1. Gastroenterology 2008: 134 (4): A306.

Sarah C. Glover, Chinmay Chauhan, Crystal L. Foster, Shruthi Bharadwaj, Ramana V. Vishnubhotla, Victor Nekrasov. Polyethylene Glycol (PEG) Prevents Against the Pro-Invasive Effects of Both Commensal and Pathogenic E. coli and May Increase Chemoresponsiveness of Colon Cancer Cells By Increasing Proliferation. Gastroenterology 2009: 136 (5 Supp 1): A321.

Sarah C. Glover, Victor Nekrasov, Ramana V. Vishnubhotla, Shruthi Bharadwaj, Crystal L. Foster. Commensal E. coli Strains Have the Ability to Alter the ECM Topography Independent of Colonic Epithelial Cells. Gastroenterology 2009: 136 (5 Supp 1): A573.

Ramana V. Vishnubhotla, Shruthi Bharadwaj, Victor Nekrasov, Sarah C. Glover. Colon Cancer and Rho Kinase: Is Rock-II Really the Most Active Rock? Gastroenterology 2010: 138 (5 Supp 1): S-736.

Sarah C. Glover, Ramana Vishnubhotla, Michael Cho, Shruthi Bharadwaj. Increased ECM Density Increases Rock's Ability to Modulate Colon Cancer Proliferation but Does Not Change Its Impact on Invasion. Gastroenterology 2011: 140 (5, Supp 1) : S-829.

PROFESSIONAL MEMBERSHIP:

American Institute of Chemical Engineers
Biomedical Engineering Society
American Gastroenterological Association
Controlled Release Society
Chicago Student Chapter Board Member – Treasurer